Review of CP Violation, with Group Formalism and the Universe

John Ronayne (10318997), Kevin Maguire (10318135), Sinead Hales(10318221), Dudley Grant (10275291)
(Dated: November 22, 2013)

Discussed in this review is the theoretical background for CP violation. This is conventionally explained through the mechanism of the CKM matrix. The mixing of quarks leads to complex phases that contribute to the so called unitary triangles. The three angles α ,β and γ that these triangles are composed of are measurable and provide information on the scale of CP violation. The CKM mechanism is a basis for calculations of weak interactions and developments of deeper understandings of CP violation in the Standard Model. Presented are the current and expected experimental verifications in three systems of particles, neutral Kaons, B mesons and in the charm sector with D mesons. In order to explain the observed antimatter asymmetry of the universe various new models of CP violation have been created, the most popular being super-symmetric or spontaneous CP violation. The gauge-symmetries of these theories can be examined abstractly to determine which types of CP violation occur. As a final note, the role that CP violation plays in modern cosmological models and it's detection via natural particle accelerators will be discussed

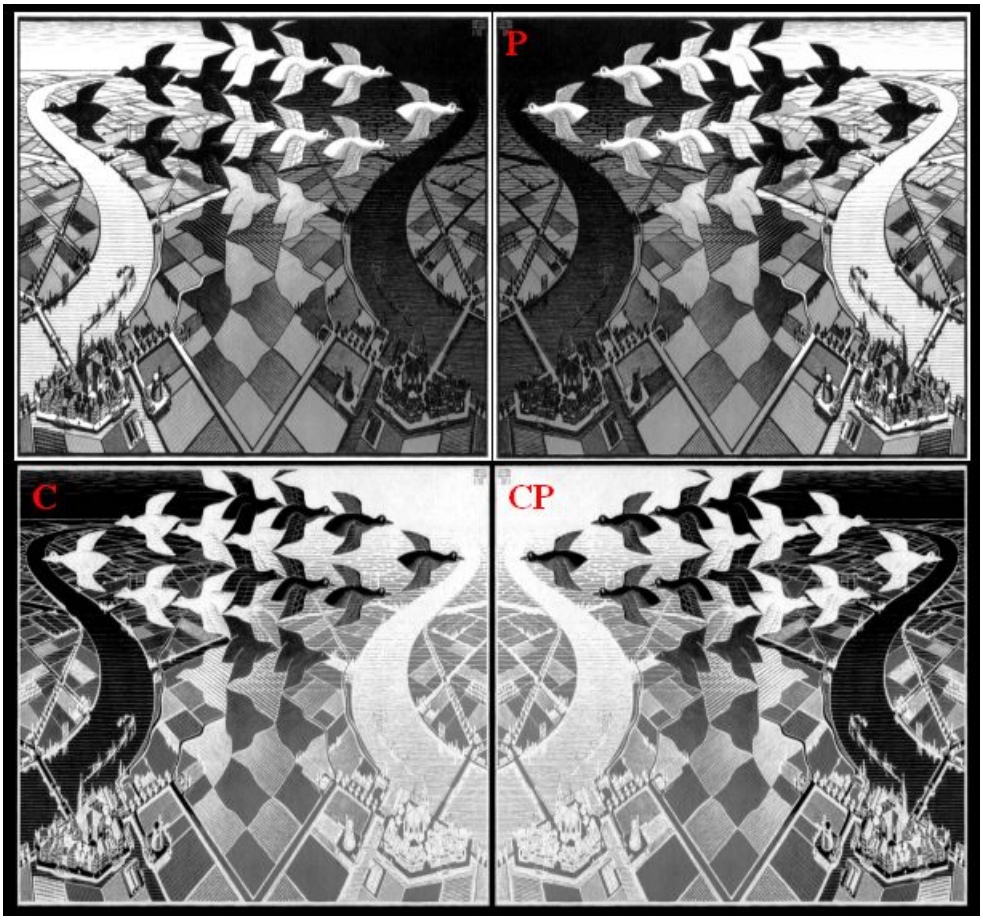

Contents

I. INTRODUCTION

A. The Parity Operator

Dudley Grant

The **parity operator**, $\hat{P}$, refers to a specific spatial reflection defined for a single particle by

$$\hat{P}\psi(\mathbf{r},t) = P\psi(-\mathbf{r},t)$$

Where $\psi(\mathbf{r},t)$ is the spatial representation of the time-evolving state $|\psi(t)\rangle$. The spatial reflection in Cartesian coordinates has matrix representation

$$\mathsf{M_{Ref}x} = \begin{pmatrix} -1 & 0 & 0 \\ 0 & -1 & 0 \\ 0 & 0 & -1 \end{pmatrix} \begin{pmatrix} x \\ y \\ z \end{pmatrix} = \begin{pmatrix} -x \\ -y \\ -z \end{pmatrix}$$

This corresponds to reflection along the plane orthogonal to the vector $\mathbf{r} = (x, y, z)$ and centred at the origin. It shall be shown $\mathsf{M_{Ref}} \in \mathrm{O}(3)$, and it forms finite a symmetry subgroup $\{\mathsf{I}, \mathsf{M_{ref}}\}$, where I is the identity matrix. This natural mathematical framework gives initial meaning to the parity operator forming a symmetry group, although really it shall be a symmetry of a Lagrangian. In this group $\mathsf{M_{Ref}}$ must be self-inverse as can easily be understood by ${\mathsf{M_{Ref}}}^2 = \mathsf{I}$. Using this

$$\begin{aligned} \hat{P}^2\psi(\mathbf{r},t) &= P\hat{P}\psi(\mathsf{M_{Ref}}\mathbf{r},t) \\ &= P^2\psi({\mathsf{M_{Ref}}}^2\mathbf{r},t) \\ &= P^2\psi(\mathsf{I}\mathbf{r},t) \\ &= P^2\psi(\mathbf{r},t) \end{aligned}$$

$P^2 = 1$ since normalisation is desired and $\psi(\mathbf{r},t)$ is normalised. Since $\hat{P}$ is chosen to be a Hermitian operator because to be able to observe its eigenvalues, its eigenvalues are real. So for an eigenstate, $\hat{P}|\psi\rangle = P|\psi\rangle$, $P = \pm 1$. For a system of n particles each in state $|\psi_i\rangle$ this definition can be extended naturally by

$$\hat{P}\left(|\psi_1\rangle \otimes |\psi_2\rangle \otimes ... \otimes |\psi_n\rangle\right) := \left(\hat{P}|\psi_1\rangle\right) \otimes \left(\hat{P}|\psi_2\rangle\right) \otimes ... \otimes \left(\hat{P}|\psi_n\rangle\right)$$

In position representation this reads more intuitively as

$$\hat{P}\psi(\mathbf{r}_1, \mathbf{r}_2, ..., \mathbf{r}_n, t) = P_1P_2...P_n\psi(-\mathbf{r}_1, -\mathbf{r}_2, ..., -\mathbf{r}_n, t)$$

Where $\mathbf{r}_i$ correspond to the spatial positions of each particle. If a Lagrangian is invariant under $\hat{P}$, that is $\mathcal{L}(\psi, \nabla\psi, x^i)$ returns the same solution as $\mathcal{L}(\hat{P}\psi, \nabla\hat{P}\psi, x^i)$, then parity is said to be conserved. This is not the case for the Standard Model. Parity may not be conserved in weak interactions.

Looking at energy eigenstates in spherical coordinates spherical harmonics, $Y_l^m(\theta,\phi)$, may be used. This gives $\phi_{nlm}(\mathbf{r}) = R_{nl}(|\mathbf{r}|)Y_l^m(\theta,\phi)$. These are essentially the Fourier modes in spherical coordinates. The parity transformation in spherical coordinates does not effect the radial distance, only the two angles. Some geometric reasoning shows that

$$\begin{pmatrix} x \\ y \\ z \end{pmatrix} \mapsto \begin{pmatrix} -x \\ -y \\ -z \end{pmatrix} \qquad \Leftrightarrow \qquad \begin{pmatrix} r \\ \theta \\ \phi \end{pmatrix} \mapsto \begin{pmatrix} r \\ \pi - \theta \\ \pi + \phi \end{pmatrix}$$

By consulting a standard textbook on special functions it can be shown that

$$Y_m^l(\theta,\phi) \mapsto Y_m^l(\pi - \theta, \pi + \phi) = (-1)^l Y_m^l(\theta,\phi)$$

For a free particle this representation is of no use. For bound systems, such as the hydrogen atom or mesons, it greatly simplifies calculation. Consider a system composed of two particles and write the effect of the parity operator on its spherical Fourier modes.

$$\begin{aligned} \hat{P}(|\phi_1\rangle \otimes |\phi_2\rangle) &= \left(\hat{P}|\phi_1\rangle\right) \otimes \left(\hat{P}|\phi_2\rangle\right) \\ &= \left(\hat{P}R_{n_1l_1}(r_1)Y_{m_1}^{l_1}(\theta_1,\phi_1)\right) \otimes \left(\hat{P}R_{n_2l_2}(r_2)Y_{m_2}^{l_2}(\theta_2,\phi_2)\right) \\ &= \left((-1)^{l_1}R_{n_1l_1}(r_1)Y_{m_1}^{l_1}(\theta_1,\phi_1)\right) \otimes \left((-1)^{l_2}R_{n_2l_2}(r_2)Y_{m_2}^{l_2}(\theta_2,\phi_2)\right) \\ &= (-1)^{l_1+l_2}|\phi_1\rangle \otimes |\phi_2\rangle \end{aligned}$$

So the parity of a spherical harmonic mode may be deduced by the total angular momentum of the system. What is left is to relate this to particle physics. This may be done by defining instrinsic parity.

A Fourier mode in Cartesian coordinates may be written in position representation as follows

$$\psi_{\mathbf{p}}(\mathbf{r},t) = e^{\frac{i}{\hbar}(\mathbf{p}\cdot\mathbf{r}-Et)}$$

This state is not physical for it is non-normalisable. $\mathbf{p}$ has interpretation as momentum of the particle. This can be checked by applying the momentum operator. Consider the parity operator's effect

$$\begin{aligned}\hat{P}\psi_{\mathbf{p}}(\mathbf{r},t) &= Pe^{\frac{i}{\hbar}(\mathbf{p}\cdot(-\mathbf{r})-Et)}\\ &= Pe^{\frac{i}{\hbar}((-\mathbf{p})\cdot\mathbf{r}-Et)}\\ &= P\psi_{-\mathbf{p}}(\mathbf{r},t)\end{aligned}$$

For $\mathbf{p}=0$ this is an eigenvalue equation. In that case, P is called the **intrinsic parity** of a particle. $\mathbf{p}=0$ may be interpreted as the particle being at rest, but as this is a non-normalisable mode it does not make sense: By the Heisenberg uncertainty principle, a quantum mechanical particle can not have an exact momentum.

In order for the Dirac equation to be symmetric under $\hat{P}$ it turns out that for an electron-positron system

$$\hat{P}(\psi_{e^-}(\mathbf{r}_-)\otimes\psi_{e^+}(\mathbf{r}_+)) = -1(\psi_{e^-}(-\mathbf{r}_-)\otimes\psi_{e^+}(-\mathbf{r}_+))$$

Now as

$$\begin{aligned}\hat{P}(\psi_{e^-}(\mathbf{r}_-)\otimes\psi_{e^+}(\mathbf{r}_+)) &= (\hat{P}\psi_{e^-}(\mathbf{r}_-))\otimes(\hat{P}\psi_{e^+}(\mathbf{r}_+))\\ &= (P_{e^-}\psi_{e^-}(-\mathbf{r}_-))\otimes(P_{e^+}\psi_{e^+}(-\mathbf{r}_+))\\ &= P_{e^-}P_{e^+}(\psi_{e^-}(-\mathbf{r}_-)\otimes\psi_{e^+}(-\mathbf{r}_+))\end{aligned}$$

This implies $P_{e^-}P_{e^+}=-1$, so depending on convention $P_{e^-}=\pm1$ and $P_{e^+}=\mp1$. The standard convention is to denote matter parity by 1 and antimatter parity by -1, so $P_{e^-}=+1$ and $P_{e^+}=-1$. It turns out this holds for any spin-$\frac{1}{2}$ particles. Using this and the spherical harmonics defined above an equation for a bound system of particles may be deduced.

First define a function $\mathsf{P}:\mathcal{H}\to\{-1,+1\}$. This function takes a state from the overall Hilbert-space of the system considered and returns the parity. For example in the electron-positron system $\mathsf{P}(|e^-\rangle\otimes|e^+\rangle)=-1$. Often this is written with the same P as the parity operator as an accepted abuse of notation. In general for a bound system of n states $|\psi_i\rangle$

$$\mathsf{P}\left(\bigotimes_{i=1}^{n}|\psi_i\rangle\right) = (-1)^{\sum_i l_i}\prod_{i=1}^{n}\mathsf{P}(|\psi_i\rangle)$$

where $\bigotimes_i|\psi_i\rangle$ is shorthand for $|\psi_1\rangle\otimes|\psi_2\rangle\otimes...\otimes|\psi_n\rangle$. Now, denoting the total angular momentum $\sum_{i=1}^{n}l_i$ by l and omitting the tensor product of states of particles this reduces to

$$\mathsf{P}\left(|p_1p_2...p_n\rangle\right) = (-1)^l\prod_{i=1}^{n}\mathsf{P}(|p_i\rangle)$$

Where p_i is short for the state of the i^{th} particle. Note that this is only true of bound states, just as free states of the hydrogen atom exist with non-discrete possible orbital angular momentum.

B. The Charge Operator

Dudley Grant

The **charge operator**, $\hat{C}$, changes a particle to its antiparticle. Intuitively, picture a particle in a certain state in the Hilbert space of states. Classically this is analogous to phase space which is the geometric space of all possible positions and velocities the particle can take, $(q^i,\dot{q}^i)$. When changed to a positron, an electron moving in phase space keeps the same position and momentum, but simply changes its sign. In other words classically all $\hat{C}$ changes the charge of a particle, but the particle keeps its direction of motion.

Consider a free electron orbiting a central positive charge, freeze this at one instant and replace with a positron. What happens? The positron accelerates away from the centre but it still keeps the tangent velocity it had originally.

In Hilbert space it is quite similar except with the addition of probabilities. If the particle is very likely to move in the $\mathbf{e_x}$ direction and $\hat{C}$ is applied, then at that instant the antiparticle is very likely to move in the $\mathbf{e_x}$ direction.

Let p represent a particle that is its own antiparticle, like the photon. Let q represent a particle that is not its own antiparticle, like a positron. The effect of $\hat{C}$ can then be described quite easily

$$\hat{C}\left|p\right\rangle = C_p\left|p\right\rangle \qquad\qquad \hat{C}\left|q\right\rangle = \left|\bar{q}\right\rangle$$

the effect of $\hat{C}^2$ should be $\hat{I}$ as changing from antiparticle and back should be invariant. This gives $C_p = \pm 1$. The reason that there is no C_q factor is: If it were introduced it does not correspond to any eigenvalue of $\hat{C}$, for antiparticles are different eigenstates. This means it cannot be measured since the definition of a quantum mechanical observable states that the observed values are eigenvalues of a hermitian operator. The arbitrary nature of C_q leads to the freedom to choose $C_q = 1$.

Generalising to a system of particles

$$\begin{aligned}\hat{C}(\left|p_1\right\rangle \otimes ... \otimes \left|p_n\right\rangle \otimes \left|q_1\right\rangle \otimes ... \otimes \left|q_m\right\rangle) &:= (\hat{C}\left|p_1\right\rangle) \otimes ... \otimes (\hat{C}\left|p_n\right\rangle) \otimes (\hat{C}\left|q_1\right\rangle) \otimes ... \otimes (\hat{C}\left|q_m\right\rangle) \\ &= (C_{p_1}\left|p_1\right\rangle) \otimes ... \otimes (C_{p_n}\left|p_n\right\rangle) \otimes \left|\bar{q}_1\right\rangle \otimes ... \otimes \left|\bar{q}_m\right\rangle \\ &= C_{p_1}...C_{p_n}\left|p_1\right\rangle \otimes ... \otimes \left|p_n\right\rangle \otimes \left|\bar{q}_1\right\rangle \otimes ... \otimes \left|\bar{q}_m\right\rangle\end{aligned}$$

In other words

$$\hat{C}\left(\bigotimes_{i=1}^{n}\left|p_i\right\rangle \otimes \bigotimes_{j=1}^{m}\left|q_j\right\rangle\right) = \prod_{i=1}^{n} C_{p_i}\left(\bigotimes_{i=1}^{n}\left|p_i\right\rangle \otimes \bigotimes_{j=1}^{m}\left|\bar{q}_j\right\rangle\right)$$

In a simplified notation this reads

$$\hat{C}\left|p_1...p_nq_1...q_m\right\rangle = C_{p_1}...C_{p_n}\left|p_1...p_n\bar{q}_1...\bar{q}_m\right\rangle$$

Like the parity operator $\hat{C}$ is also conserved under electromagnetic and strong interactions but in general is not under weak interactions.

C. The Time Reversal Operator

Dudley Grant

Time reversal is simply a reflection of the time coordinate. If the laws of physics are preserved under time reversal then while watching a video it would be impossible to tell if it were going forward and backward.

Newton's laws for conservative forces are preserved under time reversal as

$$\begin{aligned}m\mathbf{x}''(t) &= F(\mathbf{x}) \\ m\partial_t\partial_t\mathbf{x}(t) &= F(\mathbf{x})\end{aligned}$$

Change time coordinate by reflection $t \mapsto \tilde{t} := -t$, this implies $\partial_t = \frac{\partial\tilde{t}}{\partial t}\partial_{\tilde{t}} = -\partial_{\tilde{t}}$. Note $\mathbf{x}(t)$ is written in one coordinate system for time, it can also be written as $\tilde{\mathbf{x}}(\tilde{t})$ where $\tilde{\mathbf{x}}(\tilde{t}(t)) = \tilde{\mathbf{x}}(-t) = \mathbf{x}(t)$ so,

$$\begin{aligned}m(-\partial_{\tilde{t}})(-\partial_{\tilde{t}})\mathbf{x}(-\tilde{t}) &= F(\mathbf{x}) \\ m(-1)^2\partial_{\tilde{t}}\partial_{\tilde{t}}\tilde{\mathbf{x}}(\tilde{t}) &= F(\mathbf{x}) \\ m\tilde{\mathbf{x}}''(\tilde{t}) &= F(\mathbf{x})\end{aligned}$$

As the equation of motion is the same for going backward in time the symmetry has been shown.

Now in quantum mechanics consider a Fourier mode

$$\psi_{\mathbf{p}}(\mathbf{r}, t) = e^{\frac{i}{\hbar}(\mathbf{p}\cdot\mathbf{r} - Et)}$$

In classical mechanics the direction of momentum changes under time reversal as

$$\mathbf{p} = m\partial_t\mathbf{x}(t) \mapsto m(-\partial_{\tilde{t}})\mathbf{x}(-t) = -m\tilde{\mathbf{x}}(\tilde{t}) = -\tilde{\mathbf{p}}$$

In quantum mechanics it must be similar

$$\begin{aligned}\psi_{\mathbf{p}}(\mathbf{r},t) &\mapsto \psi_{-\mathbf{p}}(\mathbf{r},-t)\\ &= e^{\frac{i}{\hbar}((-\mathbf{p})\cdot\mathbf{r}-E(-t))}\\ &= \psi^*_{\mathbf{p}}(\mathbf{r},t)\end{aligned}$$

So time reversal may be represented by complex conjugate. Normalisation is preserved and so are Hermitian observables

$$\begin{aligned}|\psi(\mathbf{r},t)| \mapsto |\psi(\mathbf{r},-t)| &= |\psi^*(\mathbf{r},t)| = |\psi(\mathbf{r},t)|\\ \langle\hat{H}\rangle = \langle\psi(\mathbf{r},\mathbf{t})|\hat{H}\psi(\mathbf{r},t)\rangle &\mapsto \langle\psi^*(\mathbf{r},\mathbf{t})|\hat{H}\psi^*(\mathbf{r},t)\rangle\\ &= \langle\hat{H}^*\psi^*(\mathbf{r},\mathbf{t})|\psi^*(\mathbf{r},t)\rangle\\ &= \langle\hat{H}\psi(\mathbf{r},\mathbf{t})|\psi(\mathbf{r},t)\rangle^*\\ &= \langle\psi(\mathbf{r},\mathbf{t})|\hat{H}\psi(\mathbf{r},t)\rangle^*\\ &= \langle\psi(\mathbf{r},\mathbf{t})|\hat{H}\psi(\mathbf{r},t)\rangle\\ &= \langle\hat{H}\rangle\end{aligned}$$

Making use of the Hermitian operator's definition and that they have only real eigenvalues.

Time reversal may be a symmetry but it does not give a conservation law. For $\hat{C}$ and $\hat{P}$ it was required that they were Hermitian so their eigenvalues, $\{-1,1\}$, could be measured. One cannot define a Hermitian operator that produces the desired effects of time reversal as

$$\hat{T}\left(|\alpha\psi(t)\rangle + \beta\,|\psi(t)\rangle\right) = \alpha^*\hat{T}\,|\psi(t)\rangle + \beta^*\hat{T}\,|\psi(t)\rangle \neq \alpha\hat{T}\,|\psi(t)\rangle + \beta\hat{T}\,|\psi(t)\rangle$$

That is, $\hat{T}$ is not linear. Not only is it not hermitian it is also not an operator. Where operator is defined as a linear functional of the Hilbert space $\mathcal{H}$. As an abuse of notation it is commonly still written as $\hat{T}$.

D. CPT Theorem

Dudley Grant

The **CPT** Theorem says that any relativistic theory is symmetric under the generalised operator $\hat{C}\hat{P}\hat{T}$. In quantum theories the topic of anti-unitary operators must be introduced and explored. Essentially introducing anti-unitary operators allows to speak of "eigenvalues" of $\hat{T}$ which are $\{-1,1\}$. The details of the proof are beyond the writer's current ability and can be found here [1].

Although CPV occurs, CPT is always conserved for any physical phenomena, for a very general relativistic theory. This is the use of the theorem.

For a more detailed treatment of $\hat{C}$, $\hat{P}$ and $\hat{T}$ see [15].

E. CP and Conservation

Kevin Maguire

It has been shown that the violation of C and P are large effects. In fact, they are both maximally violated by the weak force. CP symmetry was proposed to reconcile these two quantities. This new symmetry was of course conserved by the strong and EM forces and seemed to be conserved in the weak force. There is good evidence to suggest that CP is conserved in weak decays of leptons and the helicity of neutrinos.

In considering decays of polarized muons to electron final states:

$$\mu^- \to e^-\bar{\nu}_e\nu_\mu \qquad\qquad \mu^+ \to e^+\nu_e\bar{\nu}_\mu$$

It is found that the electrons are emitted more frequently in certain directions. Thus there is an asymmetry, $\xi_\pm$ in the emission, with the two decays having different asymmetries. Under the transformation $\hat{C}$ it is expected that these

two decays would have the same asymmetry. Similarly, by the $\hat{P}$ transformation it is expected that the distributions should be completely uniform and favour no direction. It was clear that C and P were being violated, but it was also noted that μ^+ and μ^- have the exact same lifetimes. For this system CP conservation implies that the probability of an electron in one direction should be equal to the probability of a positron being emitted in the opposite direction. Using the experimentally determined formula for muon decay asymmetries it is found that CP conservation implies the $\xi_+ = -\xi_-$. Experimentally these values are measured as $\xi_+ = -\xi_- = -1.00 \pm 0.04$ [15]. Thus it is found that CP is conserved in this leptonic system. In fact, there is no experimental evidence for the violation of CP in weak leptonic decays.

The action of $\hat{C}$ and $\hat{P}$ on neutrinos with definite handedness is discussed here. Handedness, also known as helicity is defined as right if the projection of a particles spin, m_l, is in the same direction as the particles motion. This corresponds to m_l having the same sign as the particles momentum. Similarly a left handed particle has the projection of its spin in the opposite direction to its momentum. The $\hat{C}$ operator changes a particle into its anti-particle and thus a left handed neutrino transforms to a left handed anti-neutrino. The $\hat{P}$ operator reverses a particles momentum and thus changes its handedness, so a left handed neutrino goes to a right handed neutrino. However, in nature it is found that only left handed neutrinos and right handed anti-neutrinos are observed. C and P predict that decays involving left-handed neutrinos and right handed anti-neutrinos should behave the same as decays involving right handed neutrinos and left handed anti-neutrinos Thus if none of the latter are observed it is clear that these particles are not treated the same by nature, showing that C and P are violated. The solution here is that the combined operation of $\hat{C}\hat{P}$ converts a left handed neutrino to a right handed anti-neutrino, thus it is seen that CP conservation requires that only these two definite handed neutrinos are observed in nature.

This review is, of course, not on CP conservation. As stated, CP is conserved in weak leptonic decays, but this is certainly not the case in hadronic or even semi-leptonic decays. CP violation (CPV) was first observed in the mixing of neutral K-mesons by Christenson, Cronin, Fitch and Turlay in 1964 [13]. They observed the $CP = -1$ state K_L^0 decaying to 2 pions, a state with $CP = 1$. Although the fraction of K_L^0 decays violating CP in this way is tiny, the discovery was significant.

II. THE CKM MECHANISM

John Ronayne

The weak force allows the change of flavour of say an up quark to a down quark. A deeper connection in the standard model can be made when we relate this to the electron and electron neutrino transitions [9]. It was originally noted by Nicola Cabbibo that the strengths of these processes were remarkably similar to within 4%. This discrepancy however bore some real consequences. It was the assumption of the existence of a charm quark and 3rd generation of quarks by Kobayashi and Maskawa that noted this 4% uncertainty had some real significance and this difference didn't simply disappear with more accurate readings. The ability of the Weak force to decay between the generations explained this reduction in the strength of the decay amplitude. This has some rather interesting features. One can make use of Pythagoras' theorem to determine a unique angle between each decay path, known as the Cabibbo angle. If two generations were the full story we would envision that Figure 1 would be the principal triangle.

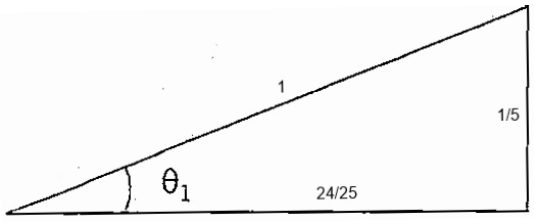

FIG. 1: Cabibbo angle θ_1. Lengths represent decay amplitudes

Only one thousandth of the 4% deviation here is accountable from the 3rd generation but for the moment lets look a bit more into the first two generations. It shall be shown that these subtle effects arising from the 3rd generation decay amplitudes are where the theory upon CP violation was developed from. From Figure 1 it is seen that the transition within a generation $u \to d$ is calculated as $\cos\theta$ and across the generation as $\sin\theta$ which actually corresponds to $u \to s$. Naively presuming only two generations of matter existed, constructing and amplitude matrix of the corresponding transitions based on this would be appropriate, as will be demonstrated in Eqn.(1). Note that, for the moment, anti-particles have amplitudes that are the same as their matter counterparts [2].

$$\begin{pmatrix} A_{ud} & A_{us} \\ A_{cd} & A_{cs} \end{pmatrix} = \begin{pmatrix} \cos\theta_1 & \sin\theta_1 \\ -\sin\theta_1 & \cos\theta_1 \end{pmatrix} \tag{1}$$

From Figure 1 it is calculated that $\theta_1 \sim 12°$. Experimentally this is measured $\theta_1 = 13.1°$ [10].The impact of this was that the decay rate of many hadronic particles could be calculated, akin to lepton decays, with the additional factor of $\cos\theta_1$or $\sin\theta_1$ in the matrix element. At a quick glance of the Weak Lagrangian,

$$\mathcal{L}_{weak} = i\bar{\psi}\gamma^{\mu}(1-\gamma^5)\partial^{\mu}\psi - q\sum \bar{\psi}\gamma^{\mu}\sigma_i(1-\gamma^5)\psi A_{\mu i} - \frac{1}{4}F_{\mu\nu}F^{\mu\nu} \tag{2}$$

the interaction term (the second term in Eqn.(2)) is a key element in the vertexes of the Feynman diagram describing the interactions in Figure 2. An element of this, γ, signifies axial vector coupling with properties which contribute to CPV [3].

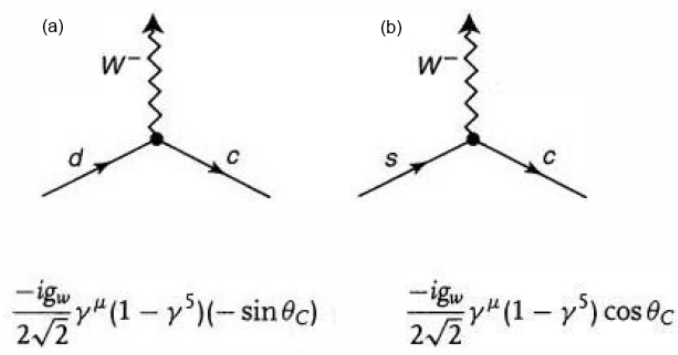

FIG. 2: Decay amplitudes across generations (Note the Cabbibo angle $\theta_c = \theta_1$). Left $d \to c$ and right $s \to c$.

To progress onto a mechanism for mixing 3 generations of quarks, the first steps must look further into what sets the weak interacting quarks apart from the quarks that are involved in electromagnetic and strong interactions. To begin let us look at an example of the Kaon decay into two muons.

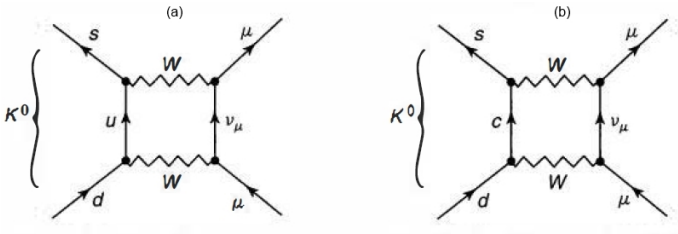

FIG. 3: Kaon Interfering Feynman diagrams illustrating GIM mechanism

So for a decay scheme as the Kaon in Figure 3.a , the virtual up quark is what will be transmitted between the down and strange. This is what would be know as a second order diagram, since the direct decay to a W boson is forbidden. When the amplitudes are found the branching ratio between that and the $K^+ \to \mu\nu$ is calculated to be,

$$\frac{K^0 \to \mu\mu}{K^+ \to \mu\nu} = 10^{-8}. \tag{3}$$

However experimentally this value is found to be too high. What could also be possible is the diagram in Figure 3.b where the virtual quark is now charm. When taking into account these two process we find that in Figure 3.a the amplitude is proportional to $\sin\theta_1\cos\theta_1$ and in Figure 3.b the amplitude is proportional to $-\sin\theta_1\cos\theta_1$ on account of A_{cd} in our simple matrix above [6]. In 1970, what is called the (Glashow, Iliopoulos and Maiani) GIM mechanism was responsible for a solution [10]. It proposed that ,through the interference with another possible decay process (or diagram) there would be a near cancellation. The remaining value came from the difference in mass between the up and charm quark. Using the experimental Amplitudes this allowed calculations and clear predictions for the mass of

the charm quark of about $1.5GeV$. It was successfully discovered in 1974 which then ushered what was known as the November Revolution [3].

Cabibbo's theory of mixing together with the GIM mechanism allows for an insightful view of quarks from a different perspective. Instead of one quark that feels the strong, electromagnetic and weak force, there is a sort of mixed phase of quarks involved in weak interactions. So an incognito weak d and s are given by,

$$d' = d\cos\theta_1 + s\sin\theta_1 \tag{4}$$

and

$$s' = s\cos\theta_1 - sin\theta_1. \tag{5}$$

This can then formulate the matrix,

$$\begin{pmatrix} d' \\ s' \end{pmatrix} = \begin{pmatrix} cos\theta_1 & sin\theta_1 \\ -sin\theta_1 & cos\theta_1 \end{pmatrix} \begin{pmatrix} d \\ s \end{pmatrix} \tag{6}$$

Now the following doublets are found like in leptons using an analogous Cabibbo rotated states,

$$\begin{pmatrix} u \\ d' \end{pmatrix} = \begin{pmatrix} u \\ d\cos\theta_1 + s\sin\theta_1 \end{pmatrix} \text{ and } \begin{pmatrix} c \\ s' \end{pmatrix} = \begin{pmatrix} c \\ s\cos\theta_1 - d\sin\theta_1 \end{pmatrix} \tag{7}$$

Moving onto a third generation of quarks, the method of finding mixing angles from the Amplitude triangles is repeated.

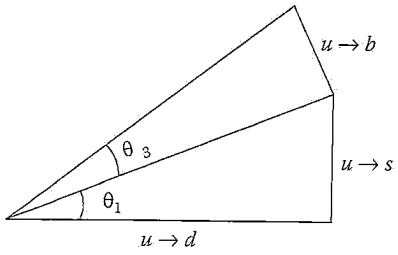

FIG. 4: Mixing triangle across 3 generations

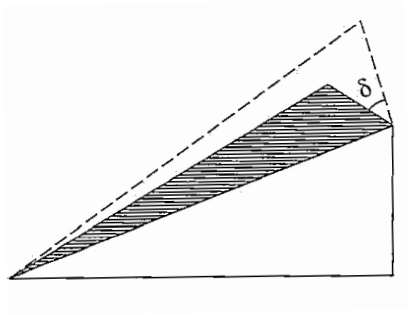

FIG. 5: Complex phase in the 2nd to 3rd generation transitions

In Figure 4 what now is in place is an additional triangle with its base atop the hypotenuse of the 1st to 2nd generation triangle. The transition now facilitates the Amplitude of the up quark transitioning towards the bottom quark path. This gives rise to the angle θ_3 a mixing angle between the 1st and 3rd generation and proceeding with this convention the mixing angle between the 2nd and 3rd is naturally θ_2. The pictorial representation has another hidden feature, Figure 6. The plane the triangle sits in can be thought of as the "matter-antimatter mirror" with

the addition freedom of the upper right-angle triangle to swing in and out of the page at an angle δ. It is called the Kobayashi-Maskawa phase, where $\delta = 0$ is on the plane of the triangle below. This parameter can set a difference between preferred taste of flavour (quarks and anti-quarks) which will later be shown in Section[IV] and may be the clue to the source of CP violation in nature and perhaps even the structure of the universe itself, but that remains to be seen since in Section[VI] and Section[VII] while still abiding to the conditions that are in place to allow for CP violation , $\delta \neq 0,\pi$ or $\theta_i \neq 0, \frac{\pi}{2}$ [5] . With a full catalogue of mixing between quarks, scaling the prior models to a 3x3 matrix is a task performed in [4] , it incorporates every type of quark mixing in the original formalism.

$$V_{CKM} = \begin{pmatrix} V_{ud} & V_{us} & V_{ub} \\ V_{cd} & V_{cs} & V_{cb} \\ V_{td} & V_{ts} & V_{tb} \end{pmatrix} = \begin{pmatrix} c_1 & s_1c_3 & s_1s_3 \\ -s_1c_2 & c_1c_2c_3 - s_2s_3e^{i\delta} & c_1c_2s_3 + s_2c_3e^{i\delta} \\ -s_1s_2 & c_1s_2c_3 + c_2s_3e^{i\delta} & c_1s_2s_3 - c_2c_3e^{i\delta} \end{pmatrix}. \tag{8}$$

In order to take advantage of the CKM matrix and illuminate CP violating decays, two weak amplitudes with complex phase components must exist. An example of such would be the model 4 quark system [5]. Consider two up quarks i and k and two down quarks j and l. Its possible to find that the matrix element is,

$$M = (V_{ij}V_{kl})A_1e^{i\delta_1} + (V_{il}V_{kj})A_2e^{i\delta_2} \tag{9}$$

Where A_1 and A_2 are real value amplitudes and each one represents a unique initial state transitioning to the same final states .The δ_1 and δ_2 are the phases due to higher order processes. The difference between them may be defined as the $\Delta\delta = \delta_1 - \delta_2$ and is known as the CP-even phase. Performing the $\hat{CP}$ operation on this matrix element a new one is obtain,

$$\overline{M} = (V_{ij}V_{kl})^*A_1e^{i\delta_1} + (V_{il}V_{kj})^*A_2e^{i\delta_2} \tag{10}$$

The two individual amplitudes A_1 and A_2 in each of the Matrix elements interfere with each other, so to simplify this down for a moment let us absorb the coefficients into A_1 and A_2 and solve for their decay rates [7]. Let,

$$|A|^2 = |A_1 + A_2|^2 = |A_1|^2 + |A_2|^2 + 2Re\,|A_2^*A_1| \tag{11}$$

$$= |A_1|^2 + |A_2|^2 + 2\,|A_1A_2|\,cos(\Delta\phi - \Delta\delta), \tag{12}$$

and

$$\left|\overline{A}\right|^2 = |A_1|^2 + |A_2|^2 + 2\,|A_1A_2|\,cos(\Delta\phi - \Delta\delta), \tag{13}$$

The ϕ in this case is the CP-even phase. Now defining the CP asymmetry as,

$$\mathbf{A}_{CP} = \frac{|A|^2 - \left|\overline{A}\right|^2}{|A|^2 + \left|\overline{A}\right|^2} \tag{14}$$

Apply equation 14 to 9 and 10 to find the Asymmetry in our four quark system we solve for the matrix elements. The result is,

$$\mathbf{M}_{CP} = \frac{2Im(\,V_{ij}\,V_{kl}\,V_{kj}^*\,V_{il}^*)\sin(\Delta\delta)A_1\,A_2}{|V_{ij}V_{kl}|^2\,A_1^2 + |V_{kj}V_{il}|^2\,A_2^2 + 2Re(\,V_{ij}\,V_{kl}\,V_{kj}^*\,V_{il}^*)\cos(\Delta\delta)A_1\,A_2} \tag{15}$$

CP violation in this respect is proportional to $2Im(\,V_{ij}\,V_{kl}\,V_{kj}^*\,V_{il}^*)$ which is called $\mathcal{J}$, the Jacobian. The Jacobian is just the gradient of the scalar valued CKM matrix it also is subject to the same CP violating conditions as what δ boasted.

So now it may same possible to be stuck with the eternal burden of having a theory with an unknown number of free parameters to test with. To fix this we would like our CKM matrix to be unitary i.e. that itself by it's complex conjugate produces the Identity matrix. A quick glance and a brief frown reveals that the matrix thus far

bare no hope unless our off-diagonal elements are relatively small. Hence since CP violation turns out to be very small experimentally and these off diagonal elements are in turn correlated to CPV it has been constructed, in close approximation, a unitary matrix as such. Adopting the Wolfenstein parametrization [11] where we expand on a small parameter $\lambda = 0.22$ to a power series,

$$V_W = \begin{vmatrix} 1-\frac{\lambda^2}{2} & \lambda & A\lambda^3(\rho - i\nu) \\ -\lambda & 1-\frac{\lambda^2}{2} & A\lambda^2 \\ A\lambda^3(1-\rho-i\nu) & -A\lambda^2 & 1 \end{vmatrix} + \mathcal{O}(\lambda^4) \tag{16}$$

Looking back at the original CKM matrix in 8,

$$\lambda = s_1 \ , \ A = \frac{s_2}{s_1^2} \ , \ \rho = \frac{s_3}{s_1 s_2}\cos\delta \text{ and } \nu = \frac{s_3}{s_1}s_2 \sin\delta.$$

Comparing this to experimentally measured values CKM matrix elements we have pretty close agreement.

$$V_{exp} = \begin{pmatrix} 0.9739-0.975 & 0.221-0.227 & 0.0029-0.0045 \\ 0.221-0.227 & 0.9730-0.9744 & 0.039-0.044 \\ 0.0048-0.01 & 0.037-0.043 & 0.9990-0.9992 \end{pmatrix} + \mathcal{O}(\lambda^4) \tag{17}$$

As you can see there is a dependence on experimental data but to what extent is it needed. An $n \times n$ complex matrix will have n^2 real and complex parameters while unitarity meaning we have n^2 constrains. Since we have 6 quarks ($2n$) which can all have independent phases we have $2n$ fewer parameters. Fixing one phase we then have $n^2 - (2n-1)$. In the real unitary matrix we have n dimensions and $\frac{n(n-1)}{2}$ free parameters. Thus the total imaginary parameters in the CKM matrix is,

$$n^2 - (2n-1) - \frac{n(n-1)}{2} = \frac{(n-1)(n-2)}{2} \tag{18}$$

which for n=3 is 1. Hence we have 4 unknown parameters in total, which is why the values of the CKM matrix depend on experimental constraints [8]

As found in [6], 9 constraints are needed, 6 of which are the sum of complex terms which are zero by orthogonality. Here are three of these unitary relation equations,

$$V_{ud}V_{us}^* + V_{cd}V_{cs}^* + V_{td}V_{ts}^* = 0, \tag{19}$$

$$V_{us}V_{ub}^* + V_{cs}V_{cb}^* + V_{ts}V_{tb}^* = 0, \tag{20}$$

$$V_{ud}V_{ub}^* + V_{cd}V_{cb}^* + V_{td}V_{tb}^* = 0, \tag{21}$$

A way to visualize these is as the Unitary triangles in the complex plane and have a surface area of $\frac{|\mathcal{J}|}{2}$ [12]. The area is then non-zero for CP violating weak interactions.

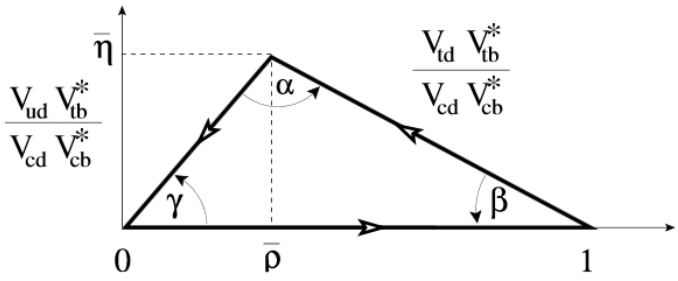

FIG. 6: Unitary Triangle with angles α, β and γ

Now to look a bit closer at the unitary Eqn.(21) to construct the appropriate triangle. In Figure 6 a triangle on the basis (x,y) with corners at (0,0), (1,0) and $(\overline{\rho}, \overline{\nu})$ is formed, where the reparameterizations are,

$$\overline{\rho} = \rho\left(1 - \frac{\lambda^2}{2}\right) \text{ and } \overline{\nu} = \nu\left(1 - \frac{\lambda^2}{2}\right) \tag{22}$$

The three angles in this diagram α, β and γ are defined as,

$$\alpha \equiv arg\left(-\frac{V_{tb}V_{tb}^*}{V_{ud}V_{ub}^*}\right) = \frac{1}{2}\sin^{-1}\left(\frac{2\overline{\nu}(\overline{\nu}^2 + \overline{\rho}^2 - \overline{\rho})}{(\overline{\rho}^2 + \overline{\nu}^2)((1-\overline{\nu})^2 + \overline{\nu}^2)}\right). \tag{23}$$

$$\beta \equiv argl\left(-\frac{V_{cd}V_{cb}^*}{V_{td}V_{tb}^*}\right) = \frac{1}{2}\sin^{-1}\left(\frac{2\overline{\nu}(1-\overline{\rho})}{(1-\overline{\rho})^2 + \overline{\rho}^2}\right). \tag{24}$$

$$\gamma \equiv arg\left(-\frac{V_{ud}V_{ub}^*}{V_{cd}V_{cb}^*}\right) = \frac{1}{2}\sin^{-1}\left(\frac{2\overline{\rho}\overline{\nu}}{\overline{\rho}^2 + \overline{\nu}^2}\right). \tag{25}$$

and $\alpha + \beta + \gamma = 180°$. Direct measurement of these angles is performed by observations of CP violations in B,D and Kaon meson decays which shall be covered in the following sections [8].

III. CPV IN KAON SYSTEM

Kevin Maguire

A. Neutral Kaon Mixing

As mentioned CPV was first observed in the neutral Kaon system. Direct and indirect CPV have been observed but it is found that the process is entirely dominated by the indirect method. Essential to these mechanisms is the mixing between the neutral Kaon and its anti-particle, corresponding to the states $|K^0\rangle$ and $|\bar{K}^0\rangle$. These have quark compositions of $d\bar{s}$ and $s\bar{d}$, respectively.

In interactions involving the strong or EM force, the quantum number strangeness, which tells us the number of strange quarks in a particle, must be conserved. For the weak force it is found that, like parity, this symmetry is not conserved. Due to this many processes forbidden for the strong and EM interactions are allowed through the weak force. This violation is what makes mixing possible. Mixing is the decay of a particle into its anti-particle and can only take place when a particle is its own anti-particle, or if the particles differ by a quantum number which is not conserved by some interaction. This is the case in neutral Kaon mixing, also know as Kaon oscillations. The neutral Kaon and its anti-particle have opposite strangeness but can decay into each other through the strangeness violating weak force. See Figure 7.

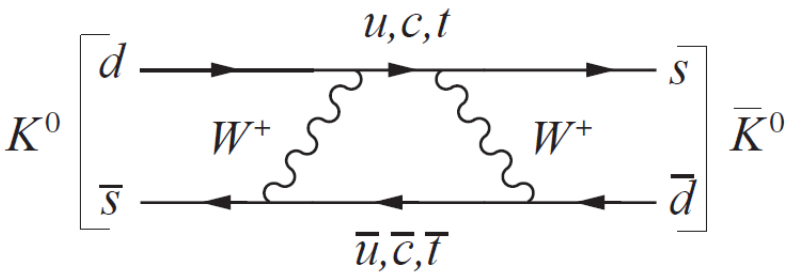

FIG. 7: *Feynmann diagram illustrating the process through which neutral Kaons decay into each other*

Analogous to the mixing of mass eigenstate quarks to different quark flavours, it is found that the neutral Kaon flavour eigenstates do not correspond to eigenstates of the $\hat{C}\hat{P}$ operator. To show this first operate on the Kaon states with $\hat{C}$. Neglecting phase throughout and assuming no CPV for now, one obtains:

$$\hat{C}\,|K^0(d\bar{s})\rangle = (1)(-1)\,|\bar{K}^0(s\bar{d})\rangle = -\,|\bar{K}^0(s\bar{d})\rangle$$
$$\hat{C}\,|\bar{K}^0(s\bar{d})\rangle = (1)(-1)\,|K^0(d\bar{s})\rangle = -\,|K^0(d\bar{s})\rangle$$

Where we have used the convention that $C(q) = 1$ and $C(\bar{q}) = -1$. Also, the action of the $\hat{P}$ operator is given by:

$$\hat{P}\,|K^0(d\bar{s})\rangle = P(d)P(\bar{s})(-1)^l\,|K^0(d\bar{s})\rangle = (1)(-1)(-1)^0\,|K^0(d\bar{s})\rangle = -\,|K^0(d\bar{s})\rangle$$
$$\hat{P}\,|\bar{K}^0(s\bar{d})\rangle = P(s)P(\bar{d})(-1)^l\,|\bar{K}^0(s\bar{d})\rangle = (1)(-1)(-1)^0\,|\bar{K}^0(s\bar{d})\rangle = -\,|\bar{K}^0(s\bar{d})\rangle$$

Where we have used the convention $P(fermion) = 1$ and $P(anti-fermion) = -1$ as well as $l = 0$ because the Kaon is the lowest energy combination of these quarks and itself has a J^P of 0^-. Now the eigenstates of $\hat{C}\hat{P}$ can be determined:

$$\hat{C}\hat{P}\,|K^0\rangle = |\bar{K}^0\rangle$$
$$\hat{C}\hat{P}\,|\bar{K}^0\rangle = |K^0\rangle$$

So it is clear that any eigenfunction of the $\hat{C}\hat{P}$ operator will be a linear combination of the two Kaon states:

$$|K_1^0\rangle = \frac{1}{\sqrt{2}}(|K^0\rangle + |\bar{K}^0\rangle) \tag{26}$$
$$|K_2^0\rangle = \frac{1}{\sqrt{2}}(|K^0\rangle - |\bar{K}^0\rangle) \tag{27}$$

Where 1 and 2 are the usual labels given to these states. Now the action of $\hat{C}\hat{P}$ on these linear combinations can be determined:

$$\hat{C}\hat{P}\,|K_1^0\rangle = \frac{1}{2}(\hat{C}\hat{P}\,|K^0\rangle + \hat{C}\hat{P}\,|\bar{K}^0\rangle) = \frac{1}{2}(|\bar{K}^0\rangle + |K^0\rangle) = |K_1^0\rangle$$
$$\hat{C}\hat{P}\,|K_2^0\rangle = \frac{1}{2}(\hat{C}\hat{P}\,|K^0\rangle - \hat{C}\hat{P}\,|\bar{K}^0\rangle) = \frac{1}{2}(|\bar{K}^0\rangle - |K^0\rangle) = -\,|K_2^0\rangle$$

In experiment, two Kaon states are observed, a short lived state denoted by $|K_S^0\rangle$ and a relatively long lived state, $|K_L^0\rangle$. The lifetimes of these particles are $(8.954 \pm 0.004) \times 10^{-11}$ s and $(5.116 \pm 0.021) \times 10^{-8}$ s, respectively [14]. We make the natural assumption that these are the $\hat{C}\hat{P}$ eigenstates just derived and the identifications $|K_S^0\rangle = |K_1^0\rangle$ and $|K_L^0\rangle = |K_2^0\rangle$, to see what is predicted. If CP is conserved then all the decays of the $|K_S^0\rangle$ ($CP = 1$) state must be to final products with $CP = 1$, and similarly, the decays of $|K_L^0\rangle$ ($CP = -1$) must be to final products with $CP = -1$. The observed decays for these states are as follows [15, pg. 292]:

$$K_S^0 \to \pi^0\pi^0 (B = 0.31), \quad K_S^0 \to \pi^+\pi^- (B = 0.69)$$
$$K_L^0 \to \pi^0\pi^0\pi^0 (B = 0.20), \quad K_L^0 \to \pi^+\pi^-\pi^0 (B = 0.13)$$

The reason for the difference in lifetimes of these two Kaon states is that the mass of the K_L^0 is not much bigger than the mass of three pions, thus it is relatively unlikely for it to undergo decay, compared to the K_S^0 which must only create energy to make two pions. The CP of these final states can now be determined. This is easy for the two pion final states. One finds:

$$P(\pi^0\pi^0) = (-1)(-1)(-1)^{l=0} = +1 \qquad \Rightarrow P = 1 \tag{28}$$
$$C(\pi^0\pi^0) = 1 \qquad \Rightarrow C = 1 \tag{29}$$
$$P(\pi^+\pi^-) = (-1)(-1)(-1)^{l=0} = +1 \qquad \Rightarrow P = 1 \tag{30}$$
$$C(\pi^+\pi^-) = (-1)^{l=0} \qquad \Rightarrow C = 1 \tag{31}$$

Thus $CP(\pi\pi) = 1$. For the three pion final state the second orbital angular momentum introduced by the third pion must be taken into account. The general formula for such a system is $P(ABC) = P(A)P(B)P(C)(-1)^{\mathbf{L}_{AB}}(-1)^{\mathbf{L}_{(AB)C}}$ where $\mathbf{L}_{AB}$ is the orbital angular momentum of the first two pions and $\mathbf{L}_{(AB)C}$ is the orbital angular momentum of the third pion with respect to the mutual centre of mass of the first two pions. See section I A. The J^P of the Kaon is 0^-, thus the overall orbital angular momentum must be zero: $\mathbf{L} = \mathbf{L}_{AB} + \mathbf{L}_{(AB)C} = 0$. As this is angular momentum addition and $\mathbf{L}$ can only take positive values, it is clear that $L_{AB} = L_{(AB)C}$ so $L_{AB} + L_{(AB)C} = 2L$, which is an even number:

$$\begin{aligned} P(\pi^0\pi^0\pi^0) =& (-1)(-1)(-1)(-1)^{2L=even} = -1 && \Rightarrow P = -1 \\ C(\pi^0\pi^0\pi^0) =& (1)(1)(1) = 1 && \Rightarrow C = +1 \\ CP(\pi^0\pi^0\pi^0) =& -1 \end{aligned}$$

For the $|\pi^+\pi^-\pi^0\rangle$ final state the parity is also -1, but the charge conjugation picks up an extra factor of $(-1)^l$ as in Eqn.(31). So if the centre of mass of pions A and B is taken to be the centre of mass between the π^+ and π^- one obtains:

$$\begin{aligned} C(\pi^+\pi^-\pi^0) =& C(\pi^0)(-1)^{L_{AB}} = 1 && \Rightarrow C = +1 \\ CP(\pi^0\pi^0\pi^0) =& -1 \end{aligned}$$

Where we set $L_{AB} = 0$ as higher L values are much less likely [16]. Thus as long as the K_L^0 decay to final states with three pions or other $CP = -1$ states and the K_S^0 only decay to two pion final states or other $CP = 1$ states, then CP is conserved.

This was thought to be the case until in 1964 when Christenson et al discovered the decay mode $K_L^0(CP = -1) \to \pi^+\pi^-(CP = 1)$ with a branching ratio of $(2.3 \pm 0.3) \times 10^{-3}$, thus discovering CPV for the first time [13]. The experiment exploits the difference in lifetimes between K_S^0 and K_L^0. A 30GeV proton beam is incident on a metal target which creates a secondary beam of many different particles. The centre of mass energy for such an arrangement is 787 MeV, which is more than enough energy to produce a neutral Kaon having about a 497 MeV rest mass. The secondary beam is passed through a magnetic field to remove any charged particles and through a 4 cm thick block of lead to remove photons. At this point the beam contains both K_S^0 and K_L^0. The detecting apparatus is placed 18 m away from the metal target, so by the time the beam reaches it, all of the K_S^0 have decayed and only K_L^0 remain. The beam is further collimated and then undergoes collisions in a helium filled bag. Two arms containing a series of detectors are mounted symmetrically around the helium bag, so they both make the same angle with the horizontal. These arms consist of a spark chamber and magnet to determine the momentum and direction of an incident particle. Water Cherenkov and scintillation detectors act as a trigger by only recording events with two oppositely charged particles and a velocity of 0.75 c to eliminate background, see Figure 8. The aim of the experiment is to measure the angular distribution of produced particles. The results of the experiment are shown in Figure 9 where N is the number of counts and θ is the angle between the net momentum of the detected particles and the initial beam direction. These measurements were taken in various mass ranges, two are shown. If $K_L^0 \to \pi^+\pi^-$ is observed, the detected particles will have opposite signs, their invariant mass will match that of $K_L^0(497)$ and their net momentum will be in the same direction as the incident beam, hence the measured angle will be zero. The results show that a peak occurs at an angle of 0° in the correct mass range. This is clear evidence of the CP violating decay $K_L^0 \to \pi^+\pi^-$.

The results of the Christensen et al experiment implies, that the weak eigenstates $|K_S^0\rangle$ and $|K_L^0\rangle$ are not aligned with the true CP eigenstates $|K_1^0\rangle$ and $|K_2^0\rangle$. As in Eqn.(26) and (27) one can write:

$$|K_S^0\rangle = a\,|K_1^0\rangle + b\,|K_2^0\rangle \tag{32}$$

$$|K_L^0\rangle = a\,|K_1^0\rangle - b\,|K_2^0\rangle \tag{33}$$

Where a and b are complex numbers. The degree to which the states are not aligned is determined using the CPV decay amplitudes and corresponding CP conserving amplitudes [18]:

$$\eta_{+-} := \frac{A(K_L^0 \to \pi^+\pi^-)}{A(K_S^0 \to \pi^+\pi^-)} = \epsilon + \epsilon'$$

$$\eta_{00} := \frac{A(K_L^0 \to \pi^0\pi^0)}{A(K_S^0 \to \pi^0\pi^0)} = \epsilon - 2\epsilon'$$

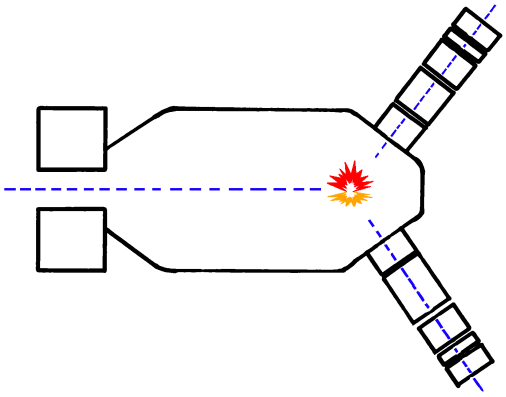

FIG. 8: *Apparatus used in the Christenson et al experiment [17]*

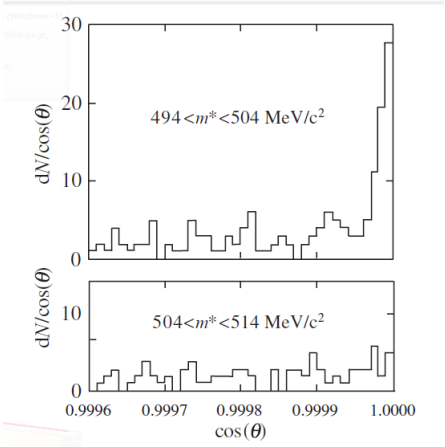

FIG. 9: *Results of the Christenson et al experiment [13]*

The two complex parameters ϵ and ϵ' determine the amount of indirect and direct CPV, respectively. The indirect CPV is due to the CP conserving decay of the $K_1^0(CP = 1)$ component of the $K_L^0(CP = -1)$ to $CP = 1$ final states, this is possible because of Kaon oscillations. The direct CPV is due to the CP violating decay of the $K_2^0(CP = -1)$ component of the $K_L^0(CP = -1)$ to $CP = 1$ final states, this is possible due to interference between different decay methods with the same final state, as in Figure 10.

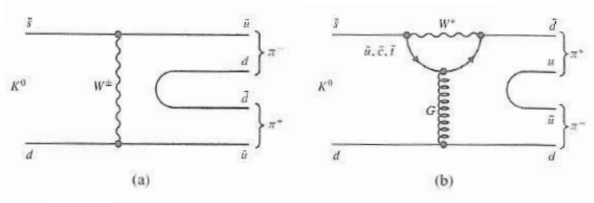

FIG. 10: *Two possible decay modes for $K^0 \to \pi^+\pi^-$. (a) Tree diagram for decay by exchanging a W boson (b) Penguin diagram for decay via quark states [19]*

However it is found that the direct CPV contribution is much smaller in this case. The indirect CPV almost completely dominates as can be seen from the similarity of the experimental values for $|\eta_{+-}|$ and $|\eta_{00}|$ [14]:

$$|\eta_{00}| = 0.002220 \pm 0.000011 \qquad |\eta_{+-}| = 0.002232 \pm 0.000011$$

If these values were significantly different it would suggest the amount of direct CPV would be comparable to the amount of indirect CPV, this of course is not the case. An experimentally determined value which illustrates this is the real part of the ratio of ϵ' to ϵ [14]:

$$\mathbb{R}\left(\frac{\epsilon'}{\epsilon}\right) = \left(1 - \left|\frac{\eta_{00}}{\eta+-}\right|\right)/3 = 0.00166 \pm 0.00023$$

$|\epsilon|$ can also be determined using:

$$|\epsilon| = \big(2|\eta_{+-}| + |\eta_{00}|\big)/3 = 0.002228 \pm 0.000011$$

If the direct CPV contributions are ignored one can write Eqn.(32) and (33) in terms of ϵ:

$$|K_L^0\rangle = \frac{1}{(1+|\epsilon|^2)^{1/2}}\Big[\epsilon\,|K_1^0\rangle + |K_2^0\rangle\Big] \tag{34}$$

$$|K_S^0\rangle = \frac{1}{(1+|\epsilon|^2)^{1/2}}\Big[|K_1^0\rangle - \epsilon\,|K_2^0\rangle\Big] \tag{35}$$

This linear combination shows the non-zero amplitude for weak eigenstate Kaons to oscillate between two different states with definite and opposite CP.

B. Semileptonic decays

Decays of neutral Kaons to products containing leptons can be used to verify Eqn.(34) and (35) as well as finding the asymmetry in the Kaon oscillation $K^0 \leftrightarrow \bar{K}^0$. First the selection rules that play an important role in these decays must be discussed.

The $\Delta S = \Delta Q$ selection rule is an empirical rule backed up by some theoretical approximations. This rules states that in decays involving strangeness(S) and leptons, the change in the charge(Q) of the hadrons must be the same as the change in strangeness which must have a value of ± 1. As an example consider semileptonic decays of the charged Σ baryon. Two semileptonic decays of this baryon are:

$$\Sigma^-(dds) \to n(udd) + e^- + \bar{\nu}_e \tag{36}$$

$$\Sigma^+(uus) \to n(udd) + e^+ + \nu_e \tag{37}$$

The Feynmann diagram for decay (36) can be drawn as in Figure 11, while decay (37) requires a diagram which must have at least two W bosons. It is clear that the diagram for Σ^- is quite likely as it contains the Cabbibo favoured quark coupling V_{ud} while any digram with two W bosons is unlikely, as for the Σ^+ decay. For this reason it is highly suppressed and has a branching ratio of $< (5 \times 10^{-6})$, which is consistent with it not existing in nature [14]. In comparison the decay (36) has a branching ratio of $(1.017 \pm 0.034) \times 10^{-3}$. As there is no selection rule forbidding the second decay, the $\Delta S = \Delta Q$ rule was introduced to identify process like it. The change in strangeness and hadron charge for these decays can be found in Table I.

TABLE I: *$\Delta S = \Delta Q$ selection rule table for the decays (36) and (37)*

Shown decay of	ΔS	ΔQ	$\Delta S = \Delta Q$
Σ^-	+1	+1	yes
Σ^+	+1	-1	no

Where ΔA is the difference between the final and initial states of A such that $\Delta A = A_{final} - A_{initial}$. Also remember that the definition of strangeness assigns the strange quark a value of -1 and the anti-strange quark a value of $+1$.

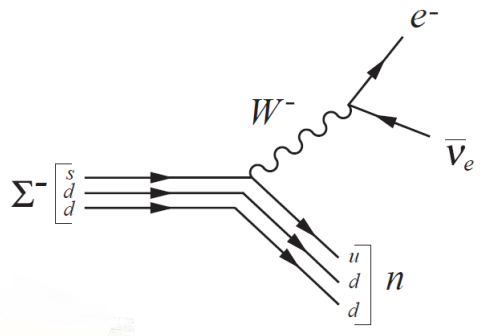

FIG. 11: *Feynmann diagram for the $\Delta s = \Delta Q$ allowed decay of the Σ^- boson to semileptonic final products*

Thus it is clear that the decay (37) violates the $\Delta S = \Delta Q$ selection rule. Similarly, a decay with $\Delta S = \pm 2$ will contain two W bosons and as a result will be very suppressed. In conclusion, $\Delta S = \Delta Q = \pm 1$ for an allowed process.

This can now be applied to semileptonic decays of Kaons of the form $K \to \pi l \nu_l$. There are four Kaon decays that have this form:

$$K^0(d\bar{s}) \to \pi^- l^+ \nu_l \tag{38}$$
$$\bar{K}^0(s\bar{d}) \to \pi^+ l^- \bar{\nu}_l \tag{39}$$
$$K^0(d\bar{s}) \to \pi^+ l^- \bar{\nu}_l \tag{40}$$
$$\bar{K}^0(s\bar{d}) \to \pi^- l^+ \nu_l \tag{41}$$

A similar table as before can now be constructed. See Table II, where the number shown refers to the equations above

TABLE II: $\Delta S = \Delta Q$ *selection rule table for the decays (38) - (41)*

Shown decay of	ΔS	ΔQ	$\Delta S = \Delta Q$
(38)	-1	-1	yes
(39)	+1	+1	yes
(40)	-1	+1	no
(41)	+1	-1	no

Thus it is clear that the only possible semileptonic decays of this form for K^0 and $\bar{K}^0$ are (38) and (39). As there is only one way for these processes to occur, there can be no interference between different processes and thus there can be no direct CP violation in the semileptonic decays of Kaons [20, pg. 10]. So it is clear that the amplitudes of the $\Delta S = \Delta Q$ violating decays are:

$$A(K^0 \to \pi^+ l^- \bar{\nu}_l) = A(\bar{K}^0 \to \pi^- l^+ \nu_l) = 0$$

It is possible now to write these amplitudes in terms of K_S^0 and K_L^0. Using Eqn.(26),(27),(34) and (35) one finds[20, pg. 11]:

$$A(K_S^0 \to \pi^+ l^- \bar{\nu}_l) = -A(K_L^0 \to \pi^+ l^- \bar{\nu}_l) = \frac{1-\epsilon}{\sqrt{2}} A(\bar{K}^0 \to \pi^+ l^- \bar{\nu}_l)$$
$$A(K_S^0 \to \pi^- l^+ \nu_l) = A(K_L^0 \to \pi^- l^+ \nu_l) = \frac{1+\epsilon}{\sqrt{2}} A(K^0 \to \pi^- l^+ \nu_l)$$

Where terms of order $|\epsilon|^2$ have been neglected. The quantities $\delta_{L,S}$ can now be defined, which show the tendency for the oscillations $K^0 \leftrightarrow \bar{K}^0$ to favour the matter particle state. Thus making a very small contribution to the matter anti-matter asymmetry

$$\delta_{L,S} = \frac{A(K^0_{L,S} \to \pi^- l^+ \nu_l) - A(K^0_{L,S} \to \pi^+ l^- \bar{\nu}_l)}{A(K^0_{L,S} \to \pi^- l^+ \nu_l) + A(K^0_{L,S} \to \pi^+ l^- \bar{\nu}_l)} := 2\mathbb{R}(\epsilon)$$

The experimental value for this quantity is $\delta_L = (3.27 \pm 0.12) \times 10^{-3}$. Which clearly indicates a small tendency to favour the matter particle in oscillations. This can also be illustrated graphically by measuring the relative number(N) of K^0 and $\bar{K}^0$ particles over time in a beam consisting initially of K^0. See Figure 12

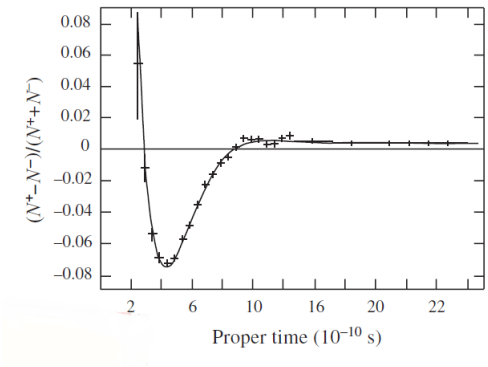

FIG. 12: *Measurements of observed Kaon semileptonic decays from a beam initially consisting of K^0 mesons which shows the oscillation between the states K^0 and $\bar{K}^0$ as well as the small asymmetry, favouring the matter particle [21]*

C. Testing CPT conservation through Strangeness Oscillations

The CPT theorem links conservation of CPT with Lorentz invariance. Thus to preserve the fundamental Lorentz symmetry physicists desperately hope CPT is conserved. Here is presented some evidence that this is indeed the case. The theorem requires particles and their anti-particles to have the same masses and lifetimes. It has been stated previously that the K^0_L and K^0_S particles have very different lifetimes, but thankfully these are not a particle anti-particle pair. From earlier it is clear that K^0 and $\bar{K}^0$ are such a pair. Thus we aim to test CPT conservation by measuring their mass difference.

By investigating the time evolution of Kaon oscillations it is possible to measure their mass difference. By inverting the linear combinations in Eqn.(26) and (27) and neglecting the very small contribution of ϵ, the flavour eigenstates are described by:

$$|K^0(t)\rangle = \frac{1}{\sqrt{2}}(|K^0_S(t)\rangle + |K^0_L(t)\rangle)$$
$$|\bar{K}^0(t)\rangle = \frac{1}{\sqrt{2}}(|K^0_S(t)\rangle - |K^0_L(t)\rangle)$$

The time evolutions of the states are then written in terms of the mass and the lifetimes of the particles

$$|K^0_S(t)\rangle = |K^0_S(0)\rangle\, e^{-(im_S + \Gamma_s/2)t}$$
$$|K^0_L(t)\rangle = |K^0_L(0)\rangle\, e^{-(im_L + \Gamma_L/2)t}$$

Where the exponential factor is as a result of the particle oscillations with time, and the fact that the particle will decay in time. We do the calculation for the $\bar{K}^0$ and simply state the result for the K^0. The probability amplitude(A) for the oscillations and then the probability of decay are determined using the linear combination:

$$|\bar{K}^0(t)\rangle = \frac{1}{\sqrt{2}}(|K_L^0(0)\rangle\, e^{-(im_L+\Gamma_L/2)t} - |K_S^0(0)\rangle\, e^{-(im_S+\Gamma_s/2)t}) \tag{42}$$

$$\bar{A} = \frac{1}{2}(e^{-(im_L+\Gamma_L/2)t} - e^{-(im_S+\Gamma_s/2)t}) \tag{43}$$

$$P(\bar{K}^0) = |\bar{A}|^2 = \frac{1}{4}\Big[e^{-\Gamma_S t} + e^{-\Gamma_L t} - 2e^{-(\Gamma_S+\Gamma_L)t/2}\cos(t\Delta m)\Big] \tag{44}$$

$$\tag{45}$$

Where $\Delta m = |m_S - m_L|$. The extra factor of $1/\sqrt{2}$ comes from the initial condition that the experiment is started with a beam of K^0 particles which is equal parts K_L^0 and K_L^0. Thus $|K_L^0(t=0)\rangle = |K_S^0(t=0)\rangle = 1/\sqrt{2}$. The corresponding probability for K^0 is as follows:

$$P(K^0) = |A|^2 = \frac{1}{4}\Big[e^{-\Gamma_S t} + e^{-\Gamma_L t} + 2e^{-(\Gamma_S+\Gamma_L)t/2}\cos(t\Delta m)\Big] \tag{46}$$

For this experiment, the initial beam of Kaons is "flavour tagged". This is done by producing the K^0 particles in a strangeness conserving strong decay. The technique of tagging will be discussed further in section [JOHNS SECTION ON B]. The strangeness of the final state particles is then determined by looking for semileptonic decays discussed in section III B. The oscillations in time are made clear by plotting Eqn.(44) and (46) in Figure 13. The decay rates for K_S^0 and K_L^0 are known so the results of this experiment can be used to determine Δm for the weak eigenstate Kaons. This value is $\Delta m = (3.483 \pm 0.006) \times 10^{-12}$.

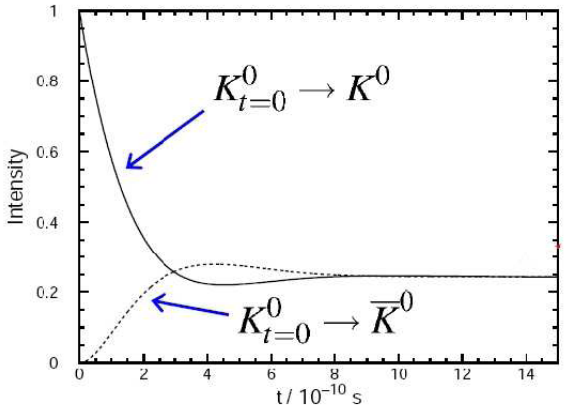

FIG. 13: *Theoretical predictions of the strangeness oscillations of a beam initially consisting of K^0 particles [22]*

To find $\Delta m_{flavour} = |m_{K^0} - m_{\bar{K}^0}|$ the link between Δm above must be determined. The time dependent asymmetry in this system is given by:

$$A_{CPT} = \frac{P[\bar{K}^0 \rightarrow \bar{K}^0(t)] - P[K^0 \rightarrow K^0(t)]}{P[\bar{K}^0 \rightarrow \bar{K}^0(t)] + P[K^0 \rightarrow K^0(t)]} = 4\mathbb{R}(\delta)$$

Where δ is a CPT violation parameter which can be written in terms of its projections parallel and perpendicular to the super weak direction $\phi_{SW} = \tan^{-1}(2\Delta m/\Delta\Gamma)$ [14]:

$$\delta_{\parallel} = \frac{1}{4}\frac{\Delta\Gamma_{flavour}}{\sqrt{\Delta m^2 + \left(\frac{\Delta\Gamma}{2}\right)^2}} \tag{47}$$

$$\delta_{\perp} = \frac{1}{2}\frac{\Delta m_{flavour}}{\sqrt{\Delta m^2 + \left(\frac{\Delta\Gamma}{2}\right)^2}} \tag{48}$$

Thus it is possible to determine $\mathbb{R}(\delta)$ in this experiment. Using other methods and other experiments $\mathbb{I}m(\delta)$ can be measured. So $\delta_{\parallel}$ and $\delta_{\perp}$ can be determined. Thus as shown in Eqn.(48) $\Delta m_{flavour}$ can be determined. The current best result for this quantity is [14]:

$$\frac{\Delta m_{flavour}}{m_{av}} < 6 \times 10^{-19}$$

which is consistent with zero. Thus this experiment gives some confidence to CPT conservation and the preservation of Lorentz invariance.

IV. B MESONS AND CPV

John Ronayne

A. Asymmetric decay rates in B meson

The neutral B meson is composed of the 1st generation down quark and a 3rd generation bottom quark. While this doesn't contrast the neutral Kaon oscillations to major extent in the preliminaries, the added benefit of the CKM mechanism is that it is clear to see why the B mesons produce a much more dramatic effect. Jumping ahead one can define the linear combinations of the B meson system with eigenfunction of $\hat{C}\hat{P}$,

$$|B_1^0\rangle = \frac{1}{\sqrt{2}}(|B^0(d\bar{b})\rangle + |\bar{B}^0(\bar{d}b)\rangle), \tag{49}$$

$$|B_2^0\rangle = \frac{1}{\sqrt{2}}(|B^0(d\bar{b})\rangle - |\bar{B}^0(\bar{d}b)\rangle), \tag{50}$$

Including mixing, it is possible to construct the two mass eigenstates,

$$|B_L\rangle = p\,|B_1^0\rangle + q\,|B_2^0\rangle\,, \tag{51}$$

$$|B_H\rangle = p\,|B_1^0\rangle - q\,|B_2^0\rangle\,, \tag{52}$$

The terminology of L for light and H for heavy in relation to the relative masses has been adopted. The mass eigenvalues can be defined by using the CKM matrix,

$$\frac{q}{p} = \frac{V_{td}^* V_{td}}{V_{td} V_{td}^*} = e^{-i2\beta} \tag{53}$$

Now the development of a few aspects of the B meson system can be seen [33]. The magnitude of $\left|\frac{q}{p}\right|$ is of interest to those whom may wish to study some direct CP. The β phase is associated to the mixing and interference and is of interest in experimental measurements of indirect CPV. First the time dependent state must be considered to provide a basis on which the coherent states may be experimentally observed and hence measured for CPV.

When experimental data is analyzed, one B meson is reconstructed fully (this includes the flavor, B or $\bar{B}$) this one is called B_{rec} with decay time t_{rec} while its sibling is inferred from the decay of the B_{rec} and is called B_{tag} with a t_{tag} decay. The time-depended Asymmetry due to CPV, in terms of $\Delta t = t_{rec} - t_{tag}$ and the number of events N, is,

$$A_{CP}(\Delta t) = \frac{N(B_{tag}^0, \Delta t) - N(\bar{B}_{tag}^0, \Delta t)}{N(B_{tag}^0, \Delta t) + N(\bar{B}_{tag}^0, \Delta t)}, \tag{54}$$

The states $|B^0\rangle$ or $|\bar{B}^0\rangle$ evolve from t=0 to a pure state of $|B_{phys}^0\rangle$ or $|\bar{B}_{phys}^0\rangle$ at great t values. These states have Decay rate eigenstates as follows,

$$|B(t)\rangle = g_+(t)\,|B^0\rangle + \left(\frac{q}{p}\right) g_-(t)\,|\bar{B}^0\rangle \tag{55}$$

$$|\bar{B}(t)\rangle = \left(\frac{p}{q}\right) g_-(t)\,|B^0\rangle + g_+(t)\,|\bar{B}^0\rangle \tag{56}$$

The complete B meson Amplitude for the decay from a $\Upsilon(4s)$ to the final product of f_{tag} or f_{rec} is,

$$g_\pm(t) = \frac{1}{2}(e^{-i\frac{\Delta m_d \Delta t}{2}} e^{-i\frac{\Delta\Gamma\Delta t}{4}} \pm e^{+i\frac{\Delta m_d \Delta t}{2}} e^{+i\frac{\Delta\Gamma\Delta t}{4}}) \tag{57}$$

Which can be shown to equal,

$$g_+(t) = e^{-iMt}e^{-\Gamma\frac{t}{2}}\cos(\Delta m_d t/2) \text{ and } g_-(t) = e^{-iMt}e^{-\Gamma\frac{t}{2}} i\sin(\Delta m_d t/2), \tag{58}$$

when $\Delta\Gamma \approx 0$, $\Delta m_d = 0.502 \pm 0.007 ps^{-1}$, $\Gamma = \frac{1}{\tau_{B^0}}$ and $M = \frac{1}{2}(M_H + M_L)$.

It is necessary to account for the antisymmetric properties of the B mesons which are produces in a P wave state when calculating coherent states Eqn.(63) [32]. To fully expand on this ,a requirement would be, that the individual amplitudes for our initialized mesons to decay to either final state. So one meson has the probability to decay to f_1 at t_1 and the other at t_2 to decay to f_2. The term Δt was mentioned before but it is of course just $\Delta t = t_1 - t_2$ and $T = t_1 + t_2$.

$$A_{1,2} = \langle f_{1,2}|\, H_{Weak}\,|B^0\rangle \text{ and } \bar{A}_{1,2} = \langle f_{1,2}|\, H_{Weak}\,|\bar{B}^0\rangle \tag{59}$$

A result which can be tested is ideal! What is possible to test then is the time-dependent rate of producing a particular decay by the term $F = \frac{\partial\Gamma}{\partial t}$ [6].

$$F(T, \Delta t) = e^{-\Gamma|\Delta t|}\,|a_+ g_+(\Delta t) + a_- g_-(\Delta(t)|^2) \tag{60}$$

the values of a_+ and a_- correspond to,

$$a_+ = \bar{A}_{tag}A_{rec} - A_{tag}\bar{A}_{rec} \text{ and } a_- = \left(-\frac{q}{p}\bar{A}_{tag}\bar{A}_{rec} + \frac{p}{q}A_{tag}A_{rec}\right) \tag{61}$$

The use of this shall now be seen but the importance to the understanding of CP violation is immense. T may be replaced by Δt which is a fundamental design capability of detector to measure, this means the physical distance of vertexes of each meson are found. As well as this the coherent states produced means that the flavor of the particle detected is fundamentally linked to the paired partner, its tag.

In a time dependent system of coherent states one often defines physical properties such as spin or polarization when dealing with light or electrons. Yet the properties ,albeit different, follow the same rules. For a system of B mesons the observables which can be examined and the apparent natural asymmetries existing are found in the eigenstates of either flavor or $\hat{CP}$.

In the case of flavor eigenstates the principle is based on mixing of coherent states. When a B meson is detected there is a quantum game of chance at play. The B_{rec} is what is seen or found through electronic signatures in the detector ,via the decay products, to be either a B^0 or $\bar{B}^0$ and its partner B_{tag} is found to be the opposite flavor, so chronologically $\bar{B}^0$ or B^0. This is what is know as an unmixed event. The time-dependent rate of decay is thus,

$$F_{unmix}(\Delta t) \propto e^{-\Gamma|\Delta t|}(1 + cos(\Delta m_d \Delta_t), \tag{62}$$

However there is the other probability. One which has show to occur is the mixing of of the two B's. Similar to spin flipping in a beam of neutrons or protons we have the flavor being flipped. The B_{rec} having been detected in a B^0 or $\bar{B}^0$ state means that the B_{tag} is in the exact same B^0 or $\bar{B}^0$ state. Giving a time-dependent rate of decay of,

$$F_{mix}(\Delta t) \propto e^{-\Gamma|\Delta t|}(1 - cos(\Delta m_d \Delta_t), \tag{63}$$

The oscillations of the B meson system is directly related to the mixing asymmetry show in Eqn.(14).

$$A_{mix}(\Delta t) = \frac{F_{unmix}(\Delta t) - F_{mix}(\Delta t)}{F_{unmix}(\Delta t) + F_{mix}(\Delta t)} = cos(\Delta m_d \Delta t) \tag{64}$$

Now to study the eigenstate of CP. Unlike before, when the concentration was in the relationship between the two decay products of B_{rec} and B_{tag}, the focus is purely on our B_{tag} as the CP eigenstate of B_{rec} is assumed. Thus the

amplitudes are found from the probable modes of decay. New the decay amplitudes are defined on the basis of the final state is accessible due to a $\hat{CP}$ operation [32].

$$A_{f_{CP}} = \langle f_{CP}| H_{Weak} |B^0\rangle \text{ and } \bar{A}_{f_{CP}} = \langle f_{CP}| H_{Weak} |\bar{B}^0\rangle \tag{65}$$

In scenario (a) the B_{tag} is decaying via a $A_{f_{CP}}$ or $\bar{A}_{f_{CP}}$ while B_{rec} decays as $A_{f_{CP}}$ and in scenario (b) B_{tag} is decaying via a $A_{f_{CP}}$ or $\bar{A}_{f_{CP}}$ while B_{rec} decays as $\bar{A}_{f_{CP}}$.

Two rates of decay arise on the pretense of the original B_{tag} flavor, these are

$$F(B_{tag} = B^0, \Delta t) \propto e^{-\Gamma|\Delta t|}\left[1 + \frac{1 - \left|\frac{q}{p}\frac{\bar{A}_{f_{CP}}}{A_{f_{CP}}}\right|^2}{1 + \left|\frac{q}{p}\frac{\bar{A}_{f_{CP}}}{A_{f_{CP}}}\right|^2}\cos(\Delta m_d \Delta t) - \frac{2Im\frac{q}{p}\frac{\bar{A}_{f_{CP}}}{A_{f_{CP}}}}{1 + \left|\frac{q}{p}\frac{\bar{A}_{f_{CP}}}{A_{f_{CP}}}\right|^2}\sin(\Delta m_d \Delta t)\right] \tag{66}$$

and,

$$F(B_{tag} = \bar{B}^0, \Delta t) \propto e^{-\Gamma|\Delta t|}\left[1 + \frac{1 - \left|\frac{q}{p}\frac{\bar{A}_{f_{CP}}}{A_{f_{CP}}}\right|^2}{1 + \left|\frac{q}{p}\frac{\bar{A}_{f_{CP}}}{A_{f_{CP}}}\right|^2}\cos(\Delta m_d \Delta t) + \frac{2Im\frac{q}{p}\frac{\bar{A}_{f_{CP}}}{A_{f_{CP}}}}{1 + \left|\frac{q}{p}\frac{\bar{A}_{f_{CP}}}{A_{f_{CP}}}\right|^2}\sin(\Delta m_d \Delta t)\right] \tag{67}$$

Again the time-dependent asymmetry was found [28] to be,

$$A_{mix}(\Delta t) = \frac{F_{B_{tag}=B^0} - F_{B_{tag}=\bar{B}^0}}{F_{B_{tag}=B^0} + F_{B_{tag}=\bar{B}^0}} = \frac{1 - \left|\frac{q}{p}\frac{\bar{A}_{f_{CP}}}{A_{f_{CP}}}\right|^2}{1 + \left|\frac{q}{p}\frac{\bar{A}_{f_{CP}}}{A_{f_{CP}}}\right|^2}\cos(\Delta m_d \Delta t) - \frac{2Im\frac{q}{p}\frac{\bar{A}_{f_{CP}}}{A_{f_{CP}}}}{1 + \left|\frac{q}{p}\frac{\bar{A}_{f_{CP}}}{A_{f_{CP}}}\right|^2}\sin(\Delta m_d \Delta t) \tag{68}$$

The shape of the decay rates are in a somewhat unique form and a definite property of the asymmetry wished to be observed, the real determination we seek is from the influence of Δt. This contributes to the amplitude, and the predicted rate which can be initially produced and detected in particle accelerators. As the measurement of such can then be compared back to Eqn.(68) to find the Unitary angle β Eqn.(24).

B. BaBar

While the decay of the Z boson at LEP was initially to study the daughter B meson particles and their asymmetry a detailed study required a more dedicated experiment and one which B meson were the sole product. What are called 'B-factories' were designed. BaBar (or $B\overline{B}$ in Stanford and Belle in Japan are experiments which create these B meson in large quantities (by large we mean 10 per second). Now focusing the attention on the BaBar experiment and in particular how it produces and detects the B mesons. The linear accelerator injects two high energy beams (electrons and positrons) into a circular collider PEP-II. Unlike most colliders the two beams are accelerated to different energies. In particular the electron beam has an energy of 9GeV and the positron beam has an energy of $3.1GeV$. The energy at the center of mass is correspondingly 10.58GeV.

At 10.58GeV it is capable of producing an $\Upsilon(4s)$ which quickly decays to either a B^+B^- or $B^0\overline{B}^0$ pair. Since the Upsilion rest mass is only just enough to create the pair the asymmetric energy beam provides the momentum to separate the pair, Figure 15. The uniqueness of this imbalance in momentum gives B mesons additional momentum upon creation relative to the laboratory center of mass frame. The benefit is that the distances the B mesons travel are then measurable and, due to time dilation induced by their high velocity, the lifetime of the B and $\overline{B}$ mesons can be determined and compared with considerable accuracy. The calculable separation that the Bs travel are on average 260um. The Upsilon's decays to the $B^0\overline{B}^0$ pair a quarter of the time, which by that is a quarter of the total hadronic cross section [citation+decay table]. Thus the luminosity of the beam needs to be significantly high to have a reliable quantity of data. The detector itself is the heart of the experiment and where some marvelous engineering and physics has been implemented to preform a detailed study of very specific decays with incredible high fidelity. The $\Upsilon(4s)$ is produced at the interaction point as shown in Figure 14. The decay products are sweep through the detector via their own momentum or under the influence of the 1.5T magnetic field produced by the superconducting coils [27].

- The Silicon Vertex Tracker(SVT) consists of five-layers of double sided silicon orientated as interlacing wafers along the inner most part of the detector. Residing only 3.2cm from the center of the 2.7cm radius beam pipe it

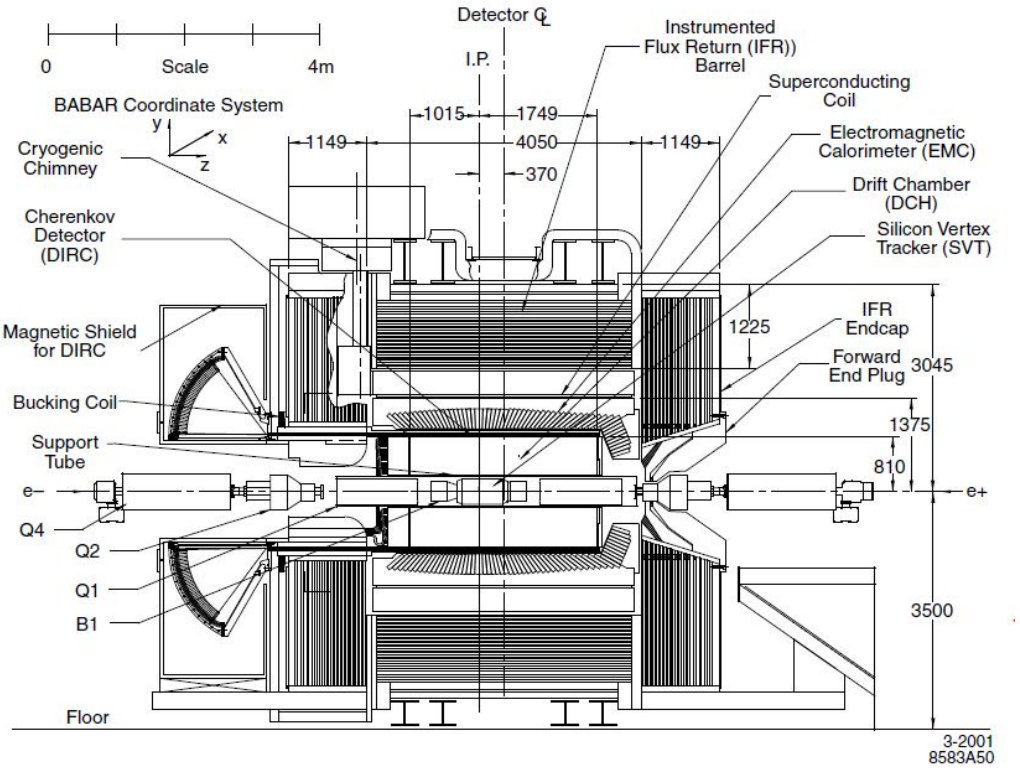

FIG. 14: The BaBar Detector Schematics

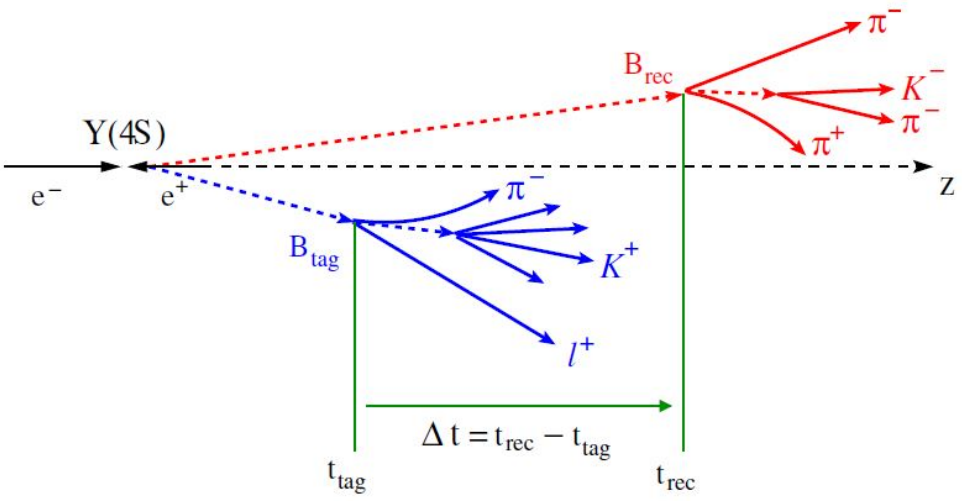

FIG. 15: $\Upsilon(4s)$ decay illustrating the crucial experimental parameter Δt

receives high fidelity detention of high energy charged particles and low energy e^+ e^- pairs to an resolution of 10 microns [36]. The primarily purpose is to contribute to the measurement of the angular and vertex information (the z and r - ϕ)of each track which corresponds to the Δz resolution where the z-axis is the parallel to the beam. The design had taken into consideration the asymmetric beam energy with the length of each layer increasing relative to the $x-y$ plane and shifted further down the z axis (along the higher energy beam path). Another design consideration to put in place was the radiation protection. Given the high luminosity of the

beam and higher probability of Coulomb scattering inside the pipe the electronic were made to withstand the near $250kRad$ per year.

- The Drift Chamber(DC) is responsible for measurements of the momentum of produced particles as well as information on identifying particles that lose energy inside (the value of dE/dt). It extends from the edge of the SVT (22cm) to a radial distance of 80cm . Inside are 7104 small cells connected to tungsten-rhenium sense wires. These wires have a 2kV potential across them and are thick enough to detect the ionized particles while keeping scattering minimal . The chamber contains a gas mixture of 20% Isobutane and 80% Helium allowing the atoms to be ionized and detected by the sense wires. [35]

- The Detector of Internally Reflected Cerenkov light (DIRC) takes advantage of the Cerenkov radiation. This is a process whereby charged particle traveling at speeds greater than the local speed of light in a medium. Silica rods are placed parallel to the beam pipe surround the outer wall of the Drift chamber. The large index of refraction ($n = 1.474$) means that the speed of light in that medium is only $0.68c$ and has a critical angle of about 43°. As charged particles enter the the silica rod and are of sufficient velocity they produce Cerenkov radiation and if it happens to be inside the critical angle it will be internally reflected along the rod to the back of the detector where they enter the "standoff box" containing water and then detected by a ring (correctly speaking a toroidal) of Photomultiplier. Reflecting "light catching cones" capture the light that might otherwise miss the PMT's active surface. The energy and incident angle of each photon is reconstructed during analysis. The primary reason to have a system as such installed is to determine between Kaons and Pions between 0.5 and $4.5GeV$, this is part of the particle Identification (PID) system.

- The EM Calorimeter's (EMC) purpose is to measure the energy and angular resolution between 20 MeV and 9 GeV. The high energy bar provides detection of the more energetic electrons, muons and photon. Slow moving neutral particles such as the π^0 and the η^0 will also be detected here. The particles rest mass energy is completely absorbed here due to interactions with the dense material. 6580 Csl(TI) (crystals grown from Csl and doped with 0.1% Thallium) trapezoidal crystals are encased in carbon fiber modules .Each Crystal is roughly the dimensions of a standard Rubix cube. Physically it extends a 0.92m to 1.27m and parallel to the pipe 2.3m downstream and 1.5m upstream from the 9GeV beam. At the longer arm length there is an endcap of crystals to facilitate the off vertical production of end products. Moreover each module is angle towards the central interaction point [37].

- The Instrument Flux Return (IFR) is separated from the EM Calorimeter by the superconducting coil and the farthest detection instrument from the Interaction point. Here muons and neutral hadrons (from the light π^0 to the heavy K_L^0 are detected with the use of the large iron structure needed as the magnetic return yoke. It is segmented into 19 hexagonal layers from 1.8m to 3m from the beam pipe. Between each layer is a single gap resistive plate chamber (RPC) which serves the purpose of detecting ionizing particles such as muon. Muons themselves are identified on the criterion of penetrating ever layer of iron, some slower muons are identified in the RPCs.

A process of particle Reconstruction and recognition from electronic signatures produced in the detector to the vast system of filtering and discriminating between background process using algorithms and triggering reveals the results to compare to theory. The time difference $\Delta t = \frac{\Delta z}{\langle \beta\gamma \rangle} c$ is obtained from the measured $\Delta z = z_1 - z_2$ and average boost $\langle \beta\gamma \rangle$ due to beam asymmetry. Since the boost is known to good precision, the Δz measurement dominates over the Δt resolution [26].

C. Experimental Evidence of *CPV* in B mesons

Testing B meson oscillations in the BaBar detector has been accomplished through the di-lepton and semi-leptonic events. An example of such a decay is $B^0 \to D^{*-} l^+ \nu$. By registering charged leptons the flavor of the decayed B meson can be calculated. Data taken at BaBar are plotted to a likelihood fit. The likelihood fit takes into account the probability of mismatched tags, the resolution of Δt and background. In Figure 16.a the unmixed decays are shown where the B meson pair are of opposite flavor while B meson pairs that have identical flavors. The mixed state are found in Figure 16.b. Finally the time dependent asymmetry of the two is found in Figure 16.c clearly exhibiting a cosine wave form as predicted, almost akin to an inference pattern an undergraduate might observe in laboratories [41]. The frequency of the B meson oscillations is 80 GHz .[23]. Noticeably the amplitude of the Mixed state is significantly lower than unmixed. The neutral mixing frequency has been measure to high accuracy at BaBar, the inclusive dilepton sample was found to be $\Delta m_d = 0.493 \pm 0.012(stat) \pm 0.009(syst) ps^{-1}$.

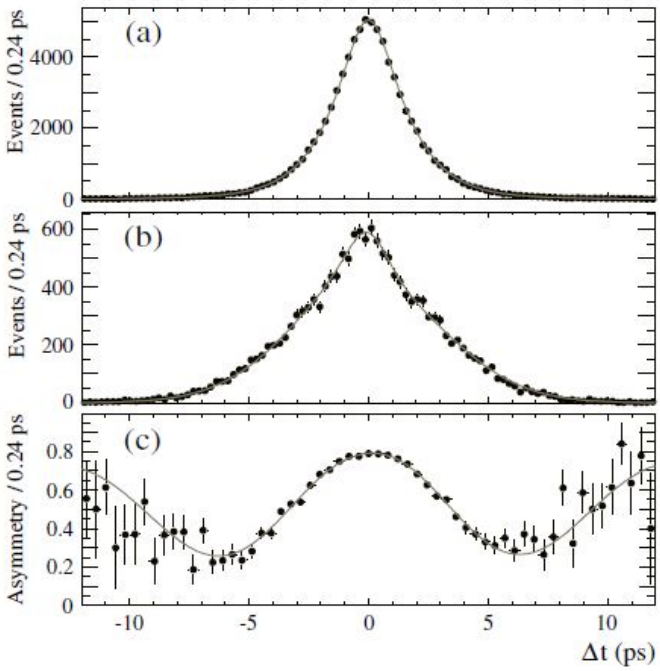

FIG. 16: (a) Unmixed flavored time dependent decay rate (b) Mixed flavored time dependent decay rate (c) Asymmetry of mixing in flavor eigenstates [23]

The CP eigenstate decay is one of the most important measurements studied. Much of the theory on CKM matrixes are easily verified by these means. It can be approximated [24] that the amplitude in Eqn.(68) can be something like,

$$\frac{q}{p}\frac{\bar{A}_{f_{CP}}}{A_{f_{CP}}} = \eta_{f_{CP}} e^{2i\beta}, \left|\frac{q}{p}\frac{\bar{A}_{f_{CP}}}{A_{f_{CP}}}\right| = 1, Im\frac{q}{p}\frac{\bar{A}_{f_{CP}}}{A_{f_{CP}}} = -\eta_{f_{CP}} \sin 2\beta \tag{69}$$

$$A_{CP} = -\eta_{f_{CP}} \sin 2\beta \sin(\Delta m_d \Delta t) \tag{70}$$

To obtain a value for the β term we focus on two elements. The Δt becomes important and allow for precision measurements of the asymmetry. The decay of interest here is $B \to J/\Upsilon K$, this is a favorable decay due to the large branching fractions ($\sim 10^{-4}$) and narrow resonance allowing a clean signal above background.[25]. In 17 the asymmetry manifesting due to CP violation is clearly visible with the data and likelihood fit corresponding to the predicted characteristics. The result for this is $\sin(2\beta) = 0.722 \pm 0.040_{stat} \pm 0.023_{syst}$. Moreover due to ambiguities in the angle β and further time depend analysis on the angular decay, $\cos(2\beta)$ is determined. The conclusion was that this is in agreement with the standard model[30][38].

Since the β angle has been determined one may now look towards finding a relevant γ term to complete the unitary triangle. The CKM phase arises from the V_{ub} term in the interferences of $b \to c$ and $b \to u$ transitions, note that the V_{cb} term is phase-less. We construct six possible Feynman diagrams for this process,

$$B^0 \to D^{*\mp}\pi^{\pm} or B^0 \to D^{*\mp}\rho^{\pm} \tag{71}$$

The first two are seen in **??**. The charged products are clean pointers to a flavor of the B_{rec} meson and it can infer the B_{tag} flavor. As per the methods used in deriving Eqn.(54) and constructing the CP asymmetry term, in terms of j, where j is only a permutation between the various end products of decay.

$$A^j_{CP}(\Delta t) = \frac{2r^j}{1 + [r^j]^2} \sin(2\beta + \gamma) cos(\delta^j) \sin(\Delta m_d \Delta t) \tag{72}$$

Since the decay [29] from $\bar{B}^0 \to D^{*+}\pi^-$, as in Figure 19, is favored via CKM mixing amplitudes over what is called the double-CKM-suppressed decay $B^0 \to D^{*+}\pi^-$ due to two low amplitude mixing terms there is a high sensitivity to the CP angle γ, Figure 18 is plot and a likelihood fit overlays the decay distribution. Since measurements of γ are

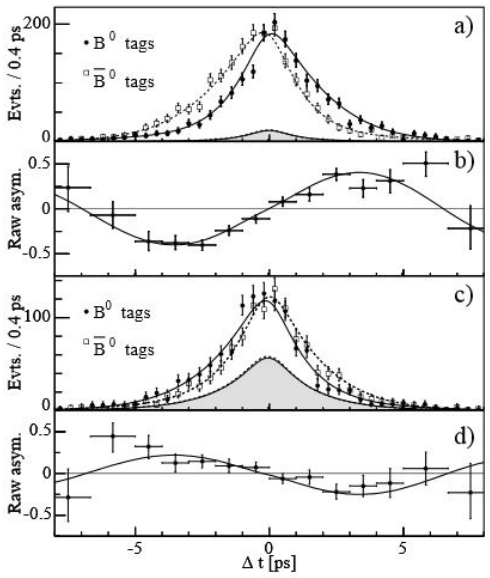

FIG. 17: (a) Time Distribution in CP odd, K_S (b) Raw Asymmetry with likelihood plot for CP odd (c) Time Distribution in CP even, K_L (d) Raw Asymmetry with likelihood plot for CP even [31]

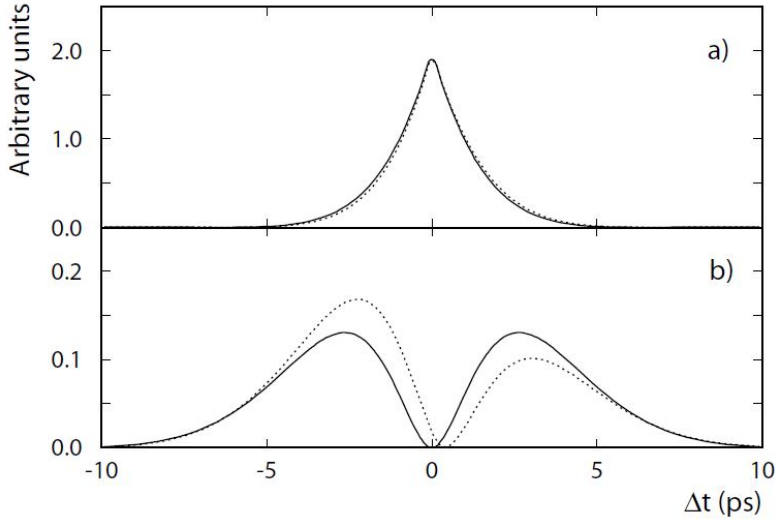

FIG. 18: (a) Time dependent decay for $\bar{B}^0 \to D^{*-}\pi^+$ (b) Time dependent decay for $B^0 \to D^{*+}\pi^-$. If no double-CKM suppression were evident the dashed line would be the amplitude.

still in their infancy the present value is $\gamma = 78° \pm 12°$. A discussion can be ignored on obtaining a value for α since no direct measurement have been successfully made, as no b quark transitions will produce such a phase. But it is possible to find a value intrinsically by the relations $\sin 2\alpha = -\sin(2\beta + 2\gamma)$.[39] .

What has been demonstrated above are the consequences of three types of CP violation. Direct being the spontaneous decay via a CP operation. Indirect being a pure asymmetry in the mixing of B-states and the combination of the spontaneous and mixing. Of these there purely indirect has never been observed as the affects are minuscule and dominated in region of high background.

The full range of angle measurement obtainable by B meson decay are shown in Figure 20 .Remarkably the validation of this particular Unitary triangle has stood up to the rigorous measurements made at BaBar. It has paved a path for the further development of new physics to provide a concrete mechanism of interactions that may lead to a fundamental understanding of this asymmetry .[40].

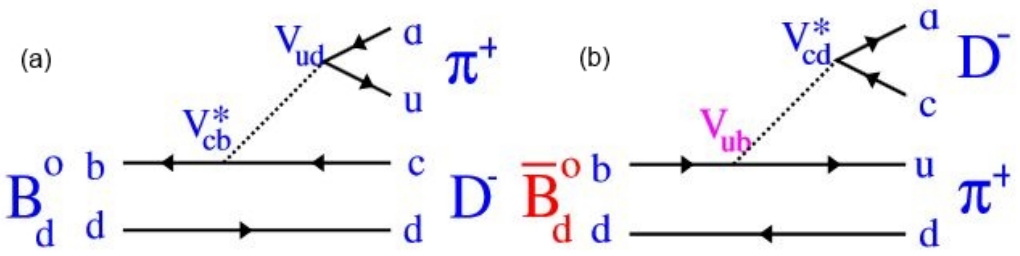

FIG. 19: (a)$B^0 \to D^-\pi^+$ and $(b)\bar{B}^0 \to D^-\pi^+$

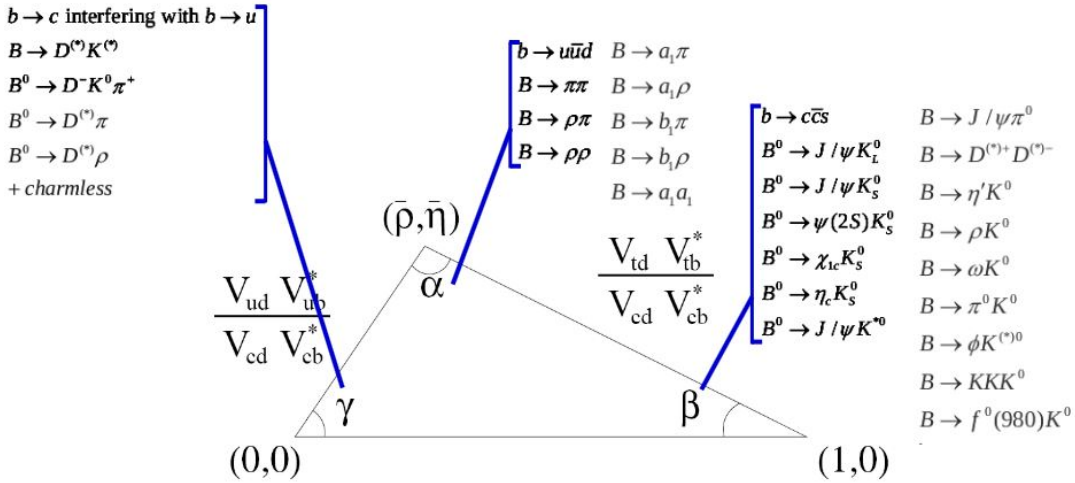

FIG. 20: The B meson Unitary triangle

V. CPV IN D MESON SYSTEM

Kevin Maguire

The quark constituents of the $D^0(1865)$ and $\bar{D}^0(1865)$ mesons are $(c\bar{u})$ and $(u\bar{c})$, respectively. This system is unique as it is the only system which undergoes mixing and contains an up-type quark. As opposed to the K^0,B^0 and B_S, which contain down quarks. This results in different quarks in the mixing box diagrams of these processes, which are illustrated in **??** and Figure 21. The rates for D^0 mixing are expected to be very small as the mixing process shown is suppressed in two ways. If the intermediate quark is a b, then the decay is doubly Cabbibo suppressed[explain? or has it been explained already?], while if the quark is a d or an s then the process is GIM suppressed, see section II. Other processes which may not have the same degree of suppression have been proposed, but there are large uncertainties in the theoretical calculations of their decay rates [45].

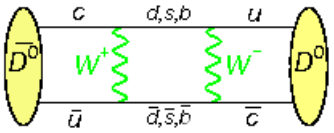

FIG. 21: *Feynmann diagram showing the process by which the two D^0 states mix. This process is the only known mixing process which contain the d,s,b quarks in this position [44]*

The first stage in detecting CPV in any system is to find mixing between a particle and its anti-particle. As in the case of Kaon and B-meson mixing we define the CP eigenstates of the D meson to be linear combinations of flavour eigenstates.

$$|D^0_{1,2}\rangle = p\,|D^0\rangle \pm q\,|\bar{D}^0\rangle \tag{73}$$

Where for normalization $|p|^2 + |q|^2 = 1$. In the absence of CPV the $|D_1\rangle$ state is a CP even state while the $|D_2\rangle$ state is a CP odd state. As expected, we will see CPV in mixing if $|p| \neq |q|$. Clear evidence for mixing between these states was announced in 2007 and published in 2008 by the BaBar collaboration, followed shortly by the Belle collaboration [42][43]. Results from both experiments show a small amount of D^0 mixing with 3.9 σ certainty, at a level which is consistent with SM predictions in the order of $|x|, |y| \leq \times 10^{-2}$, see Eqn.(74) [45]. However, measured CP violating parameters were consistent with zero, and thus with no CPV.

Two decays and their corresponding anti-particle decays are important for the measurement of mixing in the D meson system. The doubly Cabbibo suppressed (DCS) $D^0 \to K^+\pi^-$ known as the wrong sign (WS) decay and $D^0 \to K^-\pi^+$ Cabbibo favoured (CF) decay called the right sign (RS), are used. Two parameters which determine the amount of mixing in a system are defined as:

$$x = \frac{\Delta M}{\Gamma} \qquad\qquad y = \frac{\Delta\Gamma}{2\Gamma} \tag{74}$$

where $M = (M_1 + M_2)/2$ is average mass,$\Gamma = (\Gamma_1 + \Gamma_2)/2$ is average lifetime and $\Delta A := A_2 - A_1$. An approximation to the time dependence of the WS decay in the absence of CPV is given by [42]:

$$\frac{T_{WS}(t)}{e^{-\Gamma t}} \propto R_D + \sqrt{R_D} y \Gamma t + \frac{x'^2 + y'^2}{4}(\Gamma t)^2$$
$$x' = x\cos(\delta) + y\sin(\delta)$$
$$y' = y\cos(\delta) - x\sin(\delta)$$

Where R_D is the ratio of the amplitudes of the DCS decay to to CF decay and δ is the strong phase difference between the DCS and CF decays. If there is no CPV then we would expect $x' = x$ and $y' = y$. By measuring this time dependence and fitting the results to this formula, it is possible to compare predicted values of x' and y' from various theoretical models and see which best fits the data. Figure 22 shows the results of the first experiment at BaBar while Figure 23 shows more recent results from LHCb with a confidence of 5σ. Flavour tagging of the D^0 is used in these experiments. The sign of a pion known as the "slow pion" from the decay $D^{0*} \to D^0\pi^+_s$ is compared to the sign of the final product Kaon. Where D^{0*} is a heavier, and thus more energetic version of the D^0 meson. If the signs are the same, the decay is WS, if they are opposite then the decay is RS. Misidentifying a random pion - not from the D^{0*} decay - as the slow pion causes events which do not contain D^0 decays to be included in analysis. This creates a background which obstructs the signal data. Other sources of background are misreconstructed D^0 and combinatorial sources. Misreconstruction is due in part to semi-leptonic decays of the D^0 or $\bar{D}^0$ in which the detector has misidentified a lepton as a pion. Combinatorial background is caused by D mesons being produced not from D^{0*}, but from various possible decays of a B-meson. All of these backgrounds are reduced and excluded from the signal decays by making offline cuts to various parameters. These parameters include the the χ^2 of the track, vertex and impact parameters of the particles, the momentum and the mass as well as many others. Mass is plotted in two ways, the reconstructed D^0 mass distribution ($m_{K\pi}$) and the mass difference between the reconstructed D^{0*} and the D^0 mass (Δm) [46]. Signal events are identified by a mass peak in the correct place in both $m_{K\pi}$ and (Δm), random pion background has a peak in $m_{K\pi}$ but no peak in (Δm), and vice versa for misreconstructed particles. Combinatorial background has no peak in either mass distribution. These techniques are of course universal to most particle physics experiments

CPV in mixing in this system is described by the parameter A_m defined by:

$$A_m = \frac{|q/p|^2 - |p/q|^2}{|q/p|^2 + |p/q|^2}$$

Where p and q are the coefficients in the linear combinations (73). If this value is found to not be zero then CPV in D meson mixing will be proved. Similarly for direct CPV we define:

$$A_d = \frac{|A_f|^2 - |\bar{A}_f|^2}{|A_f|^2 + |\bar{A}_f|^2}$$

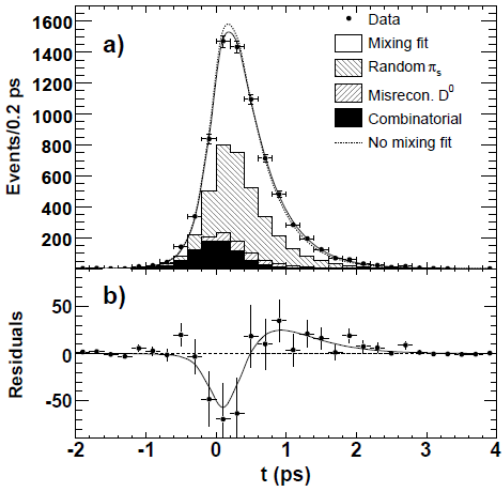

FIG. 22: *Results from the first D^0 mixing experiments at BaBar, which plots the time distribution of WS decays. It is clear that the data best fits the mixing hypothesis. Background contributions from wrongly identified π_s^+, misconstructed D^0 decays and combinatorial contributions from D^0 production from B^0 decays are removed*

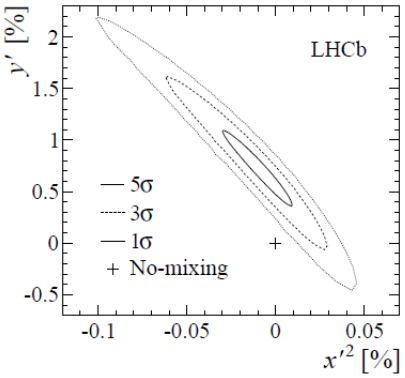

FIG. 23: *2013 Results from LHCb of D^0 mixing with a confidence of 5σ. This is the first conclusive evidence for D^0 made by one experiment The cross marks the no-mixing values of x' and y'*

Where A_f is the decay amplitude of D^0 to some final state f, and $\bar{A}_f$ is the decay amplitude of $\bar{D}^0$ to the state $\bar{f}$. These two parameters can be combined to construct the quantity λ_f defined by [48]:

$$\lambda_f = \frac{q\bar{A}_f}{pA_f} = -\eta_{CP}\left|\frac{q}{p}\right|\left|\frac{\bar{A}_f}{A_f}\right|e^{i\phi}$$

Where η_{CP} is the CP eigenvalue of the state f and ϕ is the phase between q/p and $\bar{A}_f A_f$ and is chosen by convention so that $|D_1\rangle$ is an even CP eigenstate. To date there has been no evidence for CPV in the D meson system. Measurements are ongoing at LHCb and if the addition of the 2013 data does not find evidence for CPV then we must wait till the restart of the LHC in 2015. The mush larger luminosity expected after the upgrade will hopefully supply the necessary statistics to conclusively measure a non-zero value of one of the above parameters.

VI. SPONTANEOUS CPV

Dudley Grant

A major motivation for creating models with new CPV mechanisms is to explain Baryon asymmetry. This is a huge research area, a simple search on arXiv.org reveals over 500 papers. The most prevalent theories are based around Super-Symmetry (SUSY) and Spontaneous Charge Parity Violation (SCPV).

Typically these models are created by looking for gauge symmetries which coincide with Lagrangians similar to the Standard Model, but with extra terms that may account for the preference of antimatter to decay into matter.

SCPV is praised for its "naturalness" in comparison to regular CPV[49]. It supposes the possibility to have spontaneous CPV by the vacuum, as opposed to explicit CPV from the CKM matrices. That is, the vacuum is no longer invariant under CP. In a sense this is nice as it may not introduce as many new particles. Indeed, the Minimal SUSY Standard Model is not compatible with SCPV, and in general it is difficult to incorporate SCPV in SUSY models[49], but it has been done. For example in SUSY SO(10) [50].

There are two primary goals to this section. First, to elucidate the use of groups in physics, particularly particle physics. Second, to use this knowledge to understand various SCPV models beyond the insufficient description given in this introduction.

A. Group Theory for Physics

Some physicists take pride in never having learned group theory and still understanding its applications. This is not an unreasonable point of view, an engineer can launch a rocket without knowing real analysis.

Undergraduate group theory modules quite commonly focus entirely on groups useful for pure mathematics. This is understandable as it is taught by the math department, but the picture of group theory young physicists may end up with is often quite different to its use in physics.

Part of the reasons groups can be so abstract is that they have very little structure. Even basic physics requires complicated structure. Simply changing coordinates in classical mechanics requires differential geometry, which requires analysis and topology. A **Group** is a set G with a function $\cdot : G^2 \to G$, having the following properties $\forall g, h, k \in G$

(GA1)	$g \cdot h \in G$	closure
(GA2)	$\exists e \in G,\ \ e \cdot g = g \cdot e = g$	identity
(GA3)	$\exists g^{-1} \in G,\ \ g^{-1} \cdot g = g \cdot g^{-1} = e$	inverse
(GA4)	$(g \cdot h) \cdot k = g \cdot (h \cdot k)$	associativity

Abstract definitions will be avoided in general. To understand this proceed with a useful example. Let $\mathrm{GL}(n, \mathbb{R})$ be the set of all $n \times n$ matrices with real coefficients and non-zero determinant. This forms a group under matrix multiplication.

(GA1) The product of two $n \times n$ matrices is an $n \times n$ matrix, so it is closed.

(GA2) The identity matrix I satisfies $IM = MI = M$.

(GA3) Non-zero determinant matrices are invertible $M^{-1}M = MM^{-1} = I$.

(GA4) As real multiplication and addition are associative $((1+2)+3 = 1+(2+3))$ Matrix multiplication inherits this property.

NOTE:

- The set of all real matrices would fail, as zero determinant matrices do not have inverses.
- Associativity is usually trivial by the definition and not checked.

The purpose of this proof was to give some familiar meaning to the abstraction. Detailed proofs shall be avoided in favour of intuition. Note that already a more powerful structure is present than a group, the field of real numbers, $(\mathbb{R}, +, \times)$. This is essentially just two groups glued together, addition and multiplication.

Similarly, every vector space is a group under vector addition. With this it could be said that all of physics uses groups, however a secondary school student does not use differential geometry with Newton's laws. At this stage groups are still useless to the practical physicist.

A **transformation group** is a more useful idea. Let X be a set, $\mathrm{Transf}(X)$ is the set of all one-to-one functions from X to X. This is the set of all ways of rearranging X. In the context of a finite group $S = \{1, 2, ..., n\}$, $\mathrm{Transf}(S)$ is just the set of all permutations.

If 3-dimensional space was modelled by $\mathbb{R}^3$ the transformation group would not be useful, it would contain unnatural discontinuous functions that do not relate to intuition about space. What would be useful is:

The set of transformations that preserve a property of a space form a group. It is known as the **invariance group** or the **symmetry group**.

This is an extremely general and potent idea. It is also not difficult to prove, so it shall be after the following motivation.

Model space again as $\mathbb{R}^3$, transformations should preserve distance. Where Euclidean distance is defined by

$$d(\mathbf{x},\mathbf{y}) := \sqrt{(x_1-y_1)^2+(x_2-y_2)^2+(x_3-y_3)^2}$$

The desired transformation R has form such that $d(\mathrm{R}\mathbf{x},\mathrm{R}\mathbf{y}) = d(\mathbf{x},\mathbf{y})$. From intuition there are some obvious transformations $\mathrm{R} = I$, the identity matrix, or $\mathrm{R}\mathbf{x} = \mathbf{x}+\mathbf{a}$ a translation in space

$$\begin{aligned} d(\mathrm{R}\mathbf{x},\mathrm{R}\mathbf{y}) &= d(\mathbf{x}+\mathbf{a},\mathbf{y}+\mathbf{a}) \\ &= \sqrt{\sum_{i=1}^{3}((x_i+a_i)-(y_i+a_i))^2} \\ &= \sqrt{\sum_{i=1}^{3}(x_i+a_i-y_i-a_i)^2} \\ &= \sqrt{\sum_{i=1}^{3}(x_i-y_i)^2} \\ &= d(\mathbf{x},\mathbf{y}) \end{aligned}$$

Now note

$$d(\mathbf{x},\mathbf{y})^2 = (\mathbf{x}-\mathbf{y})\cdot(\mathbf{x}-\mathbf{y})$$

Where $\cdot$ is the regular dot product. Calling $\Delta\mathbf{x} := \mathbf{x}-\mathbf{y}$ and using serif font to signify matrix representation

$$\begin{aligned} \Delta\mathbf{x}\cdot\Delta\mathbf{x} &= \Delta\mathsf{x}^T\Delta\mathsf{x} \\ &= (\mathsf{x}-\mathsf{y})^T(\mathsf{x}-\mathsf{y}) \end{aligned}$$

In other words dot product in an orthonormal basis is a row vector times a column vector. Apply the transformation and assume it preserves distance

$$(\mathrm{R}\mathsf{x}-\mathrm{R}\mathsf{y})^T(\mathrm{R}\mathsf{x}-\mathrm{R}\mathsf{y}) = (\mathsf{x}-\mathsf{y})^T(\mathsf{x}-\mathsf{y})$$

The only way this can hold for any $\mathbf{x}$ and $\mathbf{y}$ is if R is affine, $\mathrm{R}\mathbf{x} = \mathrm{A}\mathbf{x}+\mathbf{a}$ where A is linear, i.e. a Matrix,

$$\begin{aligned} (\mathrm{R}\mathsf{x}-\mathrm{R}\mathsf{y})^T(\mathrm{R}\mathsf{x}-\mathrm{R}\mathsf{y}) &= (\mathsf{x}-\mathsf{y})^T(\mathsf{x}-\mathsf{y}) \\ (\mathsf{A}\mathsf{x}+\mathsf{a}-\mathsf{A}\mathsf{y}-\mathsf{a})^T(\mathsf{A}\mathsf{x}+\mathsf{a}-\mathsf{A}\mathsf{y}-\mathsf{a}) &= (\mathsf{x}-\mathsf{y})^T(\mathsf{x}-\mathsf{y}) \\ (\mathrm{A}(\mathsf{x}-\mathsf{y}))^T(\mathrm{A}(\mathsf{x}-\mathsf{y})) &= (\mathsf{x}-\mathsf{y})^T(\mathsf{x}-\mathsf{y}) \\ (\mathrm{A}\Delta\mathsf{x})^T(\mathrm{A}\Delta\mathsf{x}) &= \Delta\mathsf{x}^T\Delta\mathsf{x} \\ \Delta\mathsf{x}^T\mathrm{A}^T\mathrm{A}\Delta\mathsf{x} &= \Delta\mathsf{x}^T\Delta\mathsf{x} \end{aligned}$$

This can only hold if $\mathsf{A}\mathsf{A}^T = I$, so $\mathsf{A}^T = \mathsf{A}^{-1}$. Immediately taking the determinant of both sides gives

$$\begin{aligned} \det\mathsf{A}\mathsf{A}^T &= \det I \\ \det\mathsf{A}\det\mathsf{A}^T &= 1 \\ \det\mathsf{A}\det\mathsf{A} &= 1 \\ \det\mathsf{A}^2 &= 1 \\ \det\mathsf{A} &\in \{-1,1\} \end{aligned}$$

This relates to intuition. The determinant of a matrix corresponds to how much it changes a volume. If the determinant of a matrix is ± 7, it will turn a 1 m^3 cube into a 7 m^3 parallelepiped, in order to preserve distance the determinant must have absolute value 1.

What sort of matrices have determinant -1 and $+1$? Consider the examples

$$\begin{pmatrix} 1 & 0 & 0 \\ 0 & -1 & 0 \\ 0 & 0 & 1 \end{pmatrix} \qquad \begin{pmatrix} 0 & -1 & 0 \\ 1 & 0 & 0 \\ 0 & 0 & 1 \end{pmatrix}$$

The left matrix represents a reflection in through the xz-plane. The right represents a rotation by $\pi/2$ in the xy-plane. It turns out that all matrices with $\mathsf{A}^T = \mathsf{A}^{-1}$ are either rotations or reflections, together they make the orthogonal group O(3). A transformation that is an orthogonal matrix plus a translation preserves distance, and the set of all such transformations form a group. Just the usual isometrics of Euclidean space.

Denote the set of rotations, which preserve length and handedness (reflection changes the right hand rule to the left hand rule), as SO(3), this is also a group.

So far this may seem over simplified but now it is already possible to define groups which preserve much more interesting and relevant properties

- Galilean Transformations. Preserve Newton's Laws.
- Unitary Operators. Preserve normalisation in quantum mechanics (QM). Propagators should have this.
- Lorentz Transformations. Preserve the light cone. Equivalently the Minkowski metric.

Intuitively, because these preserve something about a space, they form a group. This can greatly simplify some things, they are always invertible, a composition of two transformations still preserves.

There are many other aspects of group theory that can be useful here. Consider similar matrices, in the context of groups these are called conjugate elements. In the context of rotations they rotate by the same angle (but not the same direction), in the context of Lorentz Boosts they have the same speed (but not the same direction).

If the reader is interested there is a lot of literature furthering this area, particularly physics-focused is [51]. In this paper the theory shall not be explained further, aside from the symmetry group theorem proved below.

THEOREM:

Consider a set X with a function $f : X \to Y$, the set of all transformations of X that preserve the function at x,

$$S_f := \{T \in \text{Transf}(X) : f(Tx) = f(x), \forall x \in X\},$$

form a group called the ***symmetry group*** *of f.*

For the example of distance in Euclidean space, $f(Tx) = f(x)$ corresponded to $d(R\mathbf{x}, R\mathbf{y}) = d(\mathbf{x}, \mathbf{y})$.

PROOF:

(GA1) Let $S, T \in S_f$, then

$$f((ST)x) = f(S(Tx)) = f(Sx) = f(x)$$

So ST also preserves f, $ST \in S_f$.

(GA2) The identity element of e of Transf(X) satisfies $f(ex) = f(x)$ by definition of the identity function, so $e \in S_f$.

(GA3) Let $S \in S_f$. Since it is a bijection, an inverse S^{-1} exists.

$$f(S^{-1}x) = f(SS^{-1}x) = f(ex) = f(x)$$

S was introduced as it satisfies $f(Sy) = f(y)$ and pick $y = S^{-1}x$. $S^{-1} \in S_f$.

(GA4) is inherited from Transf(X). □

NOTE

- The proof of the Euclidean transformations is incomplete but trivial to extend. Assume R is affine, show it preserves distance.
- Strictly speaking symmetry groups should be considered group actions. They act on a set X, as matrices act on column vectors.

B. Useful Physical Groups

In the language of symmetry groups, useful physical transformations including the Gauge-symmetry of the Standard Model are investigated.

example 1.0 The Euclidean Isometries.

As was shown in the previous section any combination of rotation, reflection and translation preserve Euclidean distance. This can be extended to n-dimensional Euclidean space $\mathbb{E}^n$, here the group of orthogonal transformations and rotations are denoted respectively as $\mathrm{O}(n)$ and $\mathrm{SO}(n)$.

example 1.1 Galilean Transformations.

Solely preserving distance does not say much about physics. Consider Newton's laws in Cartesian coordinates in an inertial frame with column vector representation

$$m\ddot{\mathsf{x}} = \mathsf{F}$$

What sort of transformations $\mathsf{Tx} = \mathsf{Rx} + \mathsf{a}$ preserve this equation? Here R is a function of time, for example transforming to a rotating frame

$$\begin{aligned} m\frac{d^2}{dt^2}(\mathsf{Rx} + \mathsf{a}) &= \mathsf{RF} \\ m\frac{d}{dt}(\dot{\mathsf{R}}\mathsf{x} + \mathsf{R}\dot{\mathsf{x}}) + m\ddot{\mathsf{a}} &= \mathsf{RF} \\ m\frac{d}{dt}(\dot{\mathsf{R}}\mathsf{x} + \mathsf{R}\dot{\mathsf{x}}) + m\ddot{\mathsf{a}} &= \mathsf{RF} \\ m(\ddot{\mathsf{R}}\mathsf{x} + 2\dot{\mathsf{R}}\dot{\mathsf{x}} + \mathsf{R}\ddot{\mathsf{x}}) + m\ddot{\mathsf{a}} &= \mathsf{RF} \end{aligned}$$

To have the same form this requires, $\dot{R} = 0$ and $\ddot{a} = 0$. This is equivalent to saying R is a constant change of basis, such as a rotation, and $\mathsf{a} = \mathsf{v}t + \mathsf{b}$, a translation and a constant velocity. In other words

$$\mathsf{Tx} = \mathsf{Rx} + \mathsf{a}t + \mathsf{b}$$

A Galilean transformation is a symmetry group which preserves Newton's laws. It can be readily extended to also preserve distance and time intervals.

The goal is to explain the Quantum Field Theory models, Euclidean distance and Newton's Laws are not applicable. They act as an analogy for the Minkowski metric and QM.

example 2.0 Lorentz Transformations.

Suppose one wishes to preserve the Minkowski Metric, or equivalently, the light-cone. The transformations that do so are called Lorentz transformations, essentially defined by

$$\mathsf{L}^T\eta\mathsf{L} = \eta$$

Extending the transformations to allow for a translation $P^\mu_\nu x^\nu = L^\mu_\nu x^\nu + a^\mu$, these are called Poincaré transformations. The essence of Special Relativity is that the laws of physics are invariant under Poincaré transformation.

example 2.1 Unitary Transformations.

In QM the total probability of a time evolving state must always be 1, otherwise it is simply not a probabilistic theory. In the context of Hilbert spaces (complex inner product spaces complete under the induced norm), the norm of a state gives its probability, so the norm must be preserved.

Recall in Euclidean space orthogonal transformations preserve the norm of a vector, as it preserves the dot product. The complex result is analogous but in the case of operators extends far more, for example

$$|\Psi(t)\rangle = e^{-it\hat{\mathcal{H}}/\hbar}\,|\Psi(0)\rangle$$

The formal solution to the Schödinger equation, the exponential operator on the right is unitary. In general this has quite complicated form.

If the Hilbert Space is spanned by a finite set $\{|\psi_1\rangle, ..., |\psi_n\rangle\}$ it is isometrically isomorphic to the inner product space $\mathbb{C}^n$. To preserve the norm here is similar to $\mathbb{R}^n$

$$|U\mathbf{u}|^2 = (\mathsf{U}\mathsf{u})^{*T}\mathsf{U}\mathsf{u} = \mathsf{u}^{*T}\mathsf{U}^{*T}\mathsf{U}\mathsf{u} = \mathsf{u}^{*T}\mathsf{u} = |\mathbf{u}|^2$$

This holds $\forall u \in \mathbb{C}^n$ if and only if $U^{*T}U = I$. This is similar to orthogonal matrices except there is a complex conjugate. The group of all such matrices is denoted $\mathrm{U}(n)$ and those which have positive determinant form a group $\mathrm{SU}(n)$.

example 3.0 Classical Electrodynamics.

$$\nabla \cdot \mathbf{E} = \tfrac{\rho}{\varepsilon} \qquad \nabla \cdot \mathbf{B} = 0 \qquad \nabla \times \mathbf{E} = -\tfrac{\partial \mathbf{B}}{\partial t} \qquad \tfrac{1}{\mu}\nabla \times \mathbf{B} = \mathbf{j} + \varepsilon \tfrac{\partial \mathbf{E}}{\partial t}$$

As $\nabla \cdot \mathbf{B} = 0$ a theorem shows $\exists \mathbf{A}, \mathbf{B} = \nabla \times \mathbf{A}$ this together with the third equation is

$$\nabla \times \mathbf{E} = -\partial_t(\nabla \times \mathbf{E})$$
$$\nabla \times (\mathbf{E} + \frac{\partial \mathbf{A}}{\partial t}) = 0$$

Which in turn gives $\mathbf{E} = -\frac{\partial \mathbf{A}}{\partial t} - \nabla\phi$, where in the time independent case ϕ reduced to the electrostatic potential $\phi := -\int \mathbf{E} \cdot \mathrm{d}\mathbf{x}$

Consider the following transformation

$$\begin{pmatrix} \mathbf{A} \\ \phi \end{pmatrix} \mapsto \begin{pmatrix} \mathbf{A} + \nabla\lambda \\ \phi - \partial_t\lambda \end{pmatrix}$$

These transformed potentials are also valid

$$\nabla \times (\mathbf{A} + \nabla\lambda) = \nabla \times \mathbf{A} + \nabla \times \nabla \cdot \lambda = \mathbf{B} + 0$$
$$-\partial_t(\mathbf{A} + \nabla\lambda) - \nabla(\phi - \partial_t\lambda) = -\partial_t(\mathbf{A}) - \nabla\phi = \mathbf{E}$$

As these equations are preserved the gauge transformations form a symmetry group. Just as preserving Newton's laws formed a symmetry group. This is an example of a **gauge transformation**.

More generally a gauge transformation is defined as a *local* transformation that preserves the Lagrangian of a theory. What local means exactly is yet to be defined.

C. Gauge Theory

The reader may be having a hard time seeing how this relates to particle physics. With the benefit of the language being developed some light may be shed on what the remainder of this section will contain.

Most of the groups discussed have their place in modern particle physics. Lorentz invariance and unitarity of symmetry operators obviously extend from special relativity and QM. That is not all, the gauge-symmetry group of the Standard Model is $\mathrm{SU}(3) \times \mathrm{SU}(2) \times \mathrm{U}(1)$. Many of the popular extensions to the Standard Model are also defined by gauge symmetries such as SU(5), SO(10) and O(16) [52].

It is possible to state group conditions used for either (a) deducing that a theory can allow SCPV or (b) creating theories which allow for it[53]. Explaining how to use this with the mathematics being developed is the primary goal of the section. Although, the hierarchy of knowledge required for theoretical physics is unfortunately large. Despite that the material was attempted to have been presented in a condensed and tangible manner, inevitably some details will be avoided.

In QM overall phase is unimportant, that is $|\psi\rangle \sim |\psi\rangle e^{i\xi}$ where $\xi \in [0, 2\pi)$. When making any physical measurement the phase cancels out in the complex inner product. It forms a *global* gauge symmetry. Phase is still important in QM in the form of phase difference. Consider two energy eigenstates with $a, b \in \mathbb{R}$

$$|\psi\rangle = a\,|E_1\rangle\, e^{-iE_1/\hbar} + b\,|E_2\rangle\, e^{-iE_2/\hbar}$$
$$\to |\psi\rangle\, e^{iE_1/\hbar} = a\,|E_1\rangle + b\,|E_2\rangle\, e^{i(E_1 - E_2)/\hbar}$$
$$\langle \mathbf{x} \rangle = a^2\,\langle E_1|\mathbf{x}|E_1\rangle + 2ab\,\langle E_1|\mathbf{x}|E_2\rangle \cos\theta + b^2\,\langle E_2|\mathbf{x}|E_2\rangle$$

So here the phase *difference* $\theta := (E_1 - E_2)/\hbar$ appears explicitly in a measurable quantity. Compare to the phase of the CKM matrix, both phases have physical consequences. It will be shown the case is similar for SCPV. Consider U(1), a "matrix" that acts on one-dimensional complex vectors, i.e., complex numbers. In this case then, both the "matrix" and "vector" can both be represented as complex numbers

$$|uz|^2 = (uz)^* uz = u^* z^* uz = |z^2||u|^2 = |z|^2$$

This holds for all z if and only if u has length 1, so $u = e^{i\xi}$ where $\xi \in [0, 2\pi)$. So it can be said that the global phase symmetry of QM can be represented as U(1). Note that SU(1) = U(1) in this case, as the norm of a single complex number must be positive. Likewise as U(1) represents a rotation in the complex plane it must have the same group structure as SO(2). In mathematical language the groups are isomorphic, written as U(1) $\cong$ SO(2).

Thus it is clearer to say that the global phase invariance group of QM is isomorphic to U(1). Frequently it is the case that there is a deeper physical meaning behind symmetries. Merely stating a theory is invariant under U(1) is not sufficient as one must define how U(1) acts. For example, it can act globally or locally.

Consider Quantum Electrodynamics (QED) the Lagrangian of the theory is invariant under **local gauge symmetry** of U(1).

$$\psi(x^0, x^1, x^2, x^3) \mapsto e^{i\xi(x^0, x^1, x^2, x^3)} \psi(x^0, x^1, x^2, x^3)$$

Where in Cartesian coordinates $(x^0, x^1, x^2, x^3) = (ct, x, y, z)$. In shorthand

$$\psi(x) \mapsto \tilde{\psi}(x) = e^{i\xi(x)} \psi(x)$$

Where $x := (ct, x, y, z)$ This inherently insists that phase is irrelevant at any point. It was noted that more structure than merely a group is being used concerning physical groups. Fields, vector spaces, and vector calculus to name a few. Primarily calculus, a fundamentally geometric structure, appears everywhere in physics. The real scalar function $\xi(x)$ must be differentiable.

This differentiability calls for the structure of a **Lie group** (acting on a set). A Lie group is simply a group where the group operation and taking inverses are differentiable. For a simple example consider the group of addition on $\mathbb{R}$.

$$\cdot\,(x, y) = x + y \qquad\qquad \text{inv}(x) = -x$$

Both of these functions are differentiable in their arguments so $(\mathbb{R}, +)$ forms a Lie Group. Likewise other familiar groups SU(n), O(n) and GL($n, \mathbb{R}$) all form Lie groups.

To define calculus on non-Euclidean spaces the structure of differential manifolds is required. The details of which will have to be omitted but some useful properties are worth discussing. The dimension of a differential manifold is related to the intuitive understanding of spatial dimension. The surface of a sphere is a two-dimensional space and as expected forms a two-dimensional manifold. This means, for the most part, the sphere can be parametrised by two numbers (θ, ϕ).

O(n), U(n) and SU(n) have manifold dimension $\frac{1}{2}n(n-1)$, n^2 and $n^2 - 1$ respectively. So these objects are no longer purely to be considered as groups but also as abstract smooth geometric spaces.

Returning the example of QED's local gauge symmetry and comparing with the global gauge symmetry of QM

$$|\psi\rangle \mapsto |\tilde{\psi}\rangle = e^{i\xi} |\psi(x)\rangle$$
$$\psi(x) \mapsto \tilde{\psi}(x) = e^{i\xi(x)} \psi(x)$$

Both symmetries are isomorphic to U(1) but in very different contexts. In QM it may be regarded simply as a group, but in QED the differentiability effects the Lagrangian non-trivially.

The local gauge symmetry of the strong force is SU(3) and for the weak force it is SU(2). Like U(1) was represented by one parameter which was a function of space-time position $\xi(x)$, SU(2) and SU(3) have $2^2 - 1 = 3$ and $3^3 - 1 = 8$ respectively. Notice peculiarly these these are the amount of force carriers in each theory.

What do these symmetries mean physically? According to [54], they are like the the potentials $\mathbf{A}, \phi$ for classical electromagnetism; merely a tool to make the mathematics easier. In the same way as one could use $\mathbf{E}$ and $\mathbf{B}$ without the degeneracy of $\mathbf{A}$ and ϕ, in principle one could formulate QED completely independent of phase, even without complex numbers. However the difference in usability would be extreme.

A full treatment of local gauge theory for physics can be found here [54] and more on Lie groups and differential manifolds related to physics can be found in [51].

The gauge symmetries of the Standard Model are written as the product group SU(3) $\times$ SU(2) $\times$ U(1). A product group is formed in the same way $\mathbb{R}^2$ with vector addition is a product group of $\mathbb{R} \times \mathbb{R}$. This can also be considered a product manifold and indeed it tells us the number of force carriers there are in each theory. Knowing the dimension of the famous SUSY theory SU(5) is $5^2 - 1 = 24$ then tells us the number of force carriers in this theory.

One must call it at a day at some point, actually dealing with Lagrangians is a much more time consuming and worth-while task, but the language developed shall suffice to investigate SCPV models.

D. Group Theoretic Conditions

The **vacuum expectation value** (VEV) of an operator is the expected value of the operator acting on the vacuum state. A vacuum state is analogous to the lowest energy eigenstate of the quantum harmonic oscillator (QHO). For the QHO, the VEV of $\hat{\mathcal{H}}$ is $\hbar\omega/2$. Considering the ladder operators for the QHO analogously to the creation and annihilation operators in QED, this lowest energy state is equivalent to the 'no quanta' state. For the remainder of the section the vacuum state for any system shall be denoted $|0\rangle$.

In the Standard Model vacuum state in general may refer to the vacuum state of different fields. For example in the process of vacuum polarization photons may exist while the electron-positron field is in vacuum state. In order to most generally consider new models abstract scalar fields will be considered. Meaning, ϕ need not represent the wave function solely for electromagnetism. It simply represents some interesting field to a new theory.

The following is a sketch of a more rigorous development found in [53]. This paper assumes familiarity with modern Lie Group/Algebra theory and new physics models. Presented below is no substitute, but may be viewed as an intuition-based introduction through the symmetry group language developed.

Overall a theory will have a total Lagrangian $\mathcal{L}$ form that depends on every field, just like the total Lagrangian of the Standard Model. Consider first a generalised CP-transformation (GCP), denoted $\hat{G}_{CP}$, on a theory with scalar fields $\phi_i(\mathbf{x}, t)$, $i \in \{1, ..., n\}$.

$$\phi_i(\mathbf{x}, t) \mapsto U_{ij}\phi_j^*(-\mathbf{x}, t)$$

Where $[U_{ij}] =: \mathsf{U} \in \mathrm{U}(n)$, a symmetric unitary matrix. This is related to regular CP as $\hat{C}\hat{P}\phi(x) = \hat{C}\phi(-x) = c\phi^*(-x)$, where $c \in \mathbb{C}$ and ϕ is a scalar field. In column vector form we obtain

$$\begin{pmatrix} \phi_1(\mathbf{x}, t) \\ \vdots \\ \phi_n(\mathbf{x}, t) \end{pmatrix} =: \Phi(\mathbf{x}, t) \mapsto \hat{G}_{CP}\Phi(\mathbf{x}, t) = \mathsf{U}\Phi^*(-\mathbf{x}, t)$$

If the total Lagrangian is invariant under this transformation it is GCP invariant. Now the interest lies in determining the difference between explicit CPV (XCPV) and spontaneous CPV (SCPV). First it is useful to derive conditions where a model is GCP invariant.

So suppose $\mathcal{L}$ is $\hat{G}_{CP}$ invariant. Consider the Φ as a n-dimensional complex vector. By changing the basis $\Phi \mapsto \mathsf{C}\Phi$, the coordinate transformation for U is

$$\mathsf{U} \mapsto \tilde{\mathsf{U}} = \mathsf{C}\mathsf{U}\mathsf{C}^\dagger$$

Consider U temporarily as the metric for a complex inner product, by Gram-Schmidt orthonormalisation a change of basis C may be found such that $\tilde{\mathsf{U}} = \mathsf{I}$. In the context of group theory. In this new basis, then, $\hat{G}_{CP}$ reduces to

$$\Phi(\mathbf{x}, t) \mapsto \Phi^*(-\mathbf{x}, t)$$

Merely charge conjugation and reflection of space. Theories are always coordinate invariant, else they are non-physical. Hence the coordinate system $\mathsf{C}\Phi$ may be used. It has thus been shown if a theory is GCP invariant, then coordinates exist where $\mathsf{U} = \mathsf{I}$.

Explicit CPV:
Suppose that $\mathcal{L}$ is invariant under $\hat{G}_{CP}$. As was just shown, there exists a basis where $\mathsf{U} = \mathsf{I}$. Conversely, if for no $\mathsf{U} \in \mathrm{U}(n)$ is $\mathcal{L}$ invariant under $\Phi(\mathbf{x}, t) \mapsto \mathsf{U}\Phi^*(-\mathbf{x}, t)$ then the theory is explicitly CP violating. Now, this may seem to cover all cases, but, SCPV is not dependent on the GCPV condition. In fact, it is only possible to have SCPV *without* XCPV, as will be explained soon. This must immediately mean that any CPV already observed and predicted by the Standard Model must be explainable in the context of SCPV also.

Spontaneous CPV:
Suppose that $\mathcal{L}$ is invariant under $\hat{G}_{CP}$, this means XCPV cannot happen, however consider the following.

Pick a basis such that $\mathsf{U} = \mathsf{I}$. In this basis suppose that the VEVs (of the GCP operator) are not all real numbers. Depending on the VEV values it may or may not be possible to change basis again such that all the VEVs are real *and* U remains equal to I. If it is possible to find such a basis transformation, the model is totally CP-conserving. if it is not, the model has SCPV.

For a somewhat contrived but pedagogic example suppose a model has two scalar fields ϕ_1 and ϕ_2. Suppose the Lagrangian they obey is invariant under the following transformation

$$\begin{pmatrix} \phi_1(\mathbf{x},t) \\ \phi_2(\mathbf{x},t) \end{pmatrix} \mapsto \begin{pmatrix} 1 & i \\ -i & 2 \end{pmatrix} \begin{pmatrix} \phi_1^*(-\mathbf{x},t) \\ \phi_2^*(-\mathbf{x},t) \end{pmatrix}$$

This has the form of a GCP, as can be verified by checking the matrix is unitary. One can now change basis by

$$\begin{pmatrix} \phi_1(\mathbf{x},t) \\ \phi_2(\mathbf{x},t) \end{pmatrix} \mapsto \begin{pmatrix} 1 & 0 \\ i & 1 \end{pmatrix} \begin{pmatrix} \phi_1(\mathbf{x},t) \\ \phi_2(\mathbf{x},t) \end{pmatrix} = \begin{pmatrix} \phi_1(\mathbf{x},t) \\ \phi_2((x),t) + i\phi_1(\mathbf{x},t) \end{pmatrix}$$

This gives the new U by

$$\begin{pmatrix} 1 & i \\ -i & 2 \end{pmatrix} \mapsto \begin{pmatrix} 1 & 0 \\ i & 1 \end{pmatrix} \begin{pmatrix} 1 & i \\ -i & 2 \end{pmatrix} \begin{pmatrix} 1 & 0 \\ i & 1 \end{pmatrix}^\dagger = \begin{pmatrix} 1 & 0 \\ 0 & 1 \end{pmatrix}$$

So by changing the basis of the fields there is a simpler representation of GCP, it may make the overall Lagrangian more complicated, but one may simply solve that in the first coordinates for the vacuum state, then write that in the GCP preferred coordinates after.

Assume that $\mathcal{L}$ is invariant under $\hat{G}_{CP}$, that is: The Lagrangian does *not* have XCPV, unlike the Standard Model. Whether SCPV is present or not depends on the VEVs of the $\hat{G}_{CP}$ operator. To obtain these one must explicitly solve $\mathcal{L}$ and find the vacuum state, doing this abstractly one may simply choose example VEVs.

case 1 No SCPV, no XCPV.

Suppose, using the coordinate system obtained where $\mathsf{U} = \mathsf{I}$, that

$$\langle 0|\hat{G}_{CP}|0\rangle = \begin{pmatrix} \hbar\omega_1 \\ \hbar\omega_2 \end{pmatrix}$$

In this case, there is no SCPV. A coordinate basis has been founded with real VEVs and $\mathsf{U} = \mathsf{I}$.

case 2 SCPV.

Suppose, using the coordinate system obtained where $\mathsf{U} = \mathsf{I}$, that

$$\langle 0|\hat{G}_{CP}|0\rangle = \begin{pmatrix} i\hbar\omega_1 \\ \hbar\omega_2 \end{pmatrix}$$

Here it is impossible to remove the complex number and keep U as the identity matrix. So there is SCPV. So what is SCPV exactly beyond the mathematical formulation? It means the vacuum is not invariant under CP, but it is not the same CP one is used to as in the Standard Model, as for SCPV to exist XCPV must not. Returning the to earlier discussion about phase invariance in QM, for SCPV to occur one needs a *physical* phase to occur in the VEVs (for example $i = e^{i\frac{\pi}{2}}$ in the previous example). Just as the physical phase difference occurs when measuring, say, the expected value of position. So these phases do give rise to real physical meaning. Described this way, the phase of the CKM matrix is an easy analogy to understand.

> In quantum physics one must pay attention to which phases have physical consequence. Such as: (1) phase-difference between eigenstates in a quantum mechanical state, (2) the phase of the CKM matrix and (3) the relative phases of VEVs in SCPV theories.

Through the language of symmetry groups the results just obtained are powerful tools for assessing the behaviour of CP in various theories. These initial results are summarised below.

(A) Invariance of $\mathcal{L}$ under $\hat{G}_{CP}$.

(B) Having coordinates in which: (i) $\hat{G}_{CP}$ reduces to spatial reflection and conjugation and (ii) the VEVs of $\hat{G}_{CP}$ are real valued.

This leaves three interesting possibilities (as not $A \Rightarrow$ not B)

(i) (Neither A nor B) XCPV.

(ii) (A and B) SCPV.

(iii) (A and not B) Total CP invariance.

What is more interesting is painting this in more of a particle physics light. Though it is difficult to do in general as the criterion as so general it can be done by introducing new fields and therefore new particles [53]. A simplified example will be taken.

E. The Aspon Model

The theme of this section has been unravelling abstraction through examples. Continuing this trend the aspon model is explored [55]. It is an illustrative example because it is so close to the Standard Model. The local gauge symmetry of the aspon model is

$$\mathrm{SU}(3) \times \mathrm{SU}(2) \times \mathrm{U}(1) \times \mathrm{U}(1)$$

compared to the Standard Model

$$\mathrm{SU}(3) \times \mathrm{SU}(2) \times \mathrm{U}(1)$$

If two differential manifolds $\mathcal{M}$ and $\mathcal{N}$ have dimension m and n respectively, their product manifold $\mathcal{M} \times \mathcal{N}$ has dimension $m+n$. A product manifold is constructed as one would expect with the example $\mathbb{R}^2 = \mathbb{R} \times \mathbb{R}$. This means the only difference between the Standard Model's gauge symmetry group's dimension and the aspon model's is the dimension of U(1), which is $1^2 = 1$. As noted before, this corresponds to the number of force carriers in the theory which implies the aspon model has one more force carrier than the Standard Model. This force carrier is called the **aspon** and denoted A^0.

The regular Standard Model particles all have aspon charge 0. This model allows additional possible states, of most importance are two complex Higgs scalar particles denoted χ^α where $\alpha \in \{1, 2\}$, these have aspon charge 1. These are the cause of the VEV values with non-removable complex phase. In other words, here lies the SCPV.

Writing the VEVs of each new particle as

$$\langle \chi^\alpha \rangle = r_\alpha e^{i\theta_\alpha} \qquad r_\alpha \in \mathbb{R}$$

SCPV violation occurs by symmetry breaking in a manner analogous to the Higgs. These being Higgs particles allows the Higgs symmetry-breaking mechanism to be used, which causes the CPV. In turn this also gives the aspon mass.

A lot has been said in the previous paragraphs. Despite knowing the mathematical symmetry conditions required for SCPV, explicit intuition about how CPV occurs was not given. Now, with the non-removable phases appearing on Higgs particles, by symmetry breaking through the Higgs mechanism this can cause measurable CPV. Without the possibility of this symmetry breaking in SCPV theories, they would be worthless. At the very least the theories need to explain $K^0 - \bar{K}^0$ mixing and as XCPV is incompatible with SCPV, it *must* use the SCPV mechanism.

Generalisations of the aspon model are easy to construct and are the de-facto presentation in [53]. It is possible to understand what was meant by SCPV being more "natural" than XCPV in [49], simply by thinking that the symmetry breaking mechanism of the Higgs is more natural than the CKM matrix.

These generalisations simply rely on creating new fields and observing whether or not they have non-removable complex phases in VEVs and their physical effect after symmetry breaking. To be totally general the symmetry breaking need not be Higgs, but for all intents and purposes it usually will be.

In these generalised theories, the particles generated are called "spurions" of which the χ^α Higgs particles are specific examples of. SCPV is always related to symmetry breaking of the U(1) lie group, otherwise, despite VEV having complex phase, it will not show physically. Another important point is the requirement for at least two spurions, for even if there were a non-removable vacuum value like

$$\langle 0 | \hat{G}_{CP} | 0 \rangle = re^{i\theta}$$

As there is only one, this phase will never turn up measurably, one requires a phase difference (just as in QM) for it to be physical.

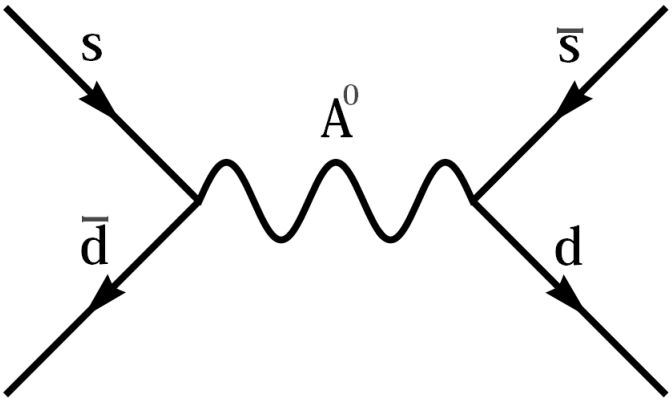

FIG. 24: *Feynman Diagram for Kaon mixing in aspon theory*

F. Summary and Application

Despite in general having quite an abstract formulation, SCPV is quite an interesting competitor for explaining CPV. Unfortunately, the mathematical details remain beyond the comprehension of the writer's current abilities. Hence, interesting ideas like exactly how new states are predicted have not been attempted. Still, seeing how complex ideas in particle physical physics can be represented by simple symmetry conditions, just as complex ideas can be represented by Feynman diagrams, makes it a far more approachable subject for an undergraduate.

As what has been discussed is such a general condition it is quite robust to how long it may remain experimentally unfalsifiable. This is not an attractive quality. One condition for falsification would be if XCPV is found to be necessary, as that would contradict the result of part D. What are perhaps more interesting are explicit SCPV theories which make falsifiable predictions. For example the aspon model makes the prediction that for K^0 mixing the CP parameters must $Re(\frac{\epsilon'}{\epsilon}) \leq 10^{-5}$ [55]. Comparing this to the experimental result given in the Neutral Kaon Mixing section, $Re(\frac{\epsilon'}{\epsilon}) = 0.00166 \pm 0.00023$ it is seen that the aspon method *has* been falsified.

Quite a few modern theories are difficult if nigh on impossible to falsify. It is refreshing to have dealt with an idea that has been proven wrong. Still, SCPV remains in many other prominent models. Aspon theory is introduced purely as an explanatory example.

VII. CONCLUSION

This review has presented the current state of CPV through the CKM theory, experimental evidence, group formalism and cosmological models. The CKM mechanism is a suitable candidate to calculate and predict weak decay modes across generations of quarks. The asymmetry between matter and antimatter is an important consequence. Testing of the CKM angles through the decays of mesons have verified the Unitary angles through experiments at BaBar. Through an understanding of 3 forms of CP violating procedures, B-mesons have provided a clean measurements of α and β verifying the CKM theory and evidence for a significant level of CP violation. As shown the first evidence for CPV in the neutral Kaon systems and subsequent discoveries in this sector are important verifications of CPV theory and also verify CPT conservation. The current state of CPV in the charm sector has been discussed, showing that current measurements are not accurate enough to verify CPV in this system. A criterion determining possible CPV mechanisms for new physical models has been introduced, highlighting the physical consequences of symmetry in nature. In particular the Aspon model and some of its experimental predictions were shown to contradict recent experimental data. During a cosmological phase transition the magnetic helicity density is related to the cosmic baryon number density and from this the CP violation responsible for the excess of matter over antimatter also provides helicity to the magnetic field.

VIII. EVIDENCE FOR CP-VIOLATION IN RELATION TO COSMOLOGICAL MODELS AND DETECTION VIA NATURAL PARTICLE ACCELERATORS

Sinead Hales

A. Justification of the hot big bang model

Consider our observable universe and it's contents, from scales to clusters of galaxies to the dust particles in between them, there appears to be a clear matter dominance over anti-matter, an asymmetry between the two. However from this asymmetry a contraction arise from the early big bang theory. One of the explanation for this discrepancy is CP violation, the combination of the C, Charge Conjugation, and P, Parity operators. It is throughout this chapter that CP violations involvement with the matter dominance in the early universe and its applications to cosmology will be investigated.

The hot big bang model is one of the most widely accepted theory for the origin of our universe among the scientific community due to its empirical merits [56][65], however a naive or simplistic model is insufficient to explain the matter anti-matter asymmetry and it could be tempting to disregard this hypothesis. The model hypothesizes that the universe as we know it was born in an explosion of tremendous proportions and despite the mentioned inconsistencies, today there exist three main observations supporting this model.[65]

- The Hubble expansion.
  The concept of the expanding universe is one that the distance between any two point changes over time, the space itself expands rather than the objects themselves away once one another. A consequences of this effect is that, as light travels through this expanding space, its wavelength is also stretched. Consider the optical component of the electromagnetic spectrum, red light has a longer wavelength than blue, as the fabric of the universe expands, as does the wavelength of the light, hence light from distant objects appears more red, this process is known as red-shifting and the longer light travels through expanding space, the more redshifting it experiences. [56] [65] Therefore, since light travels at a fixed speed, the big bang theory tells us that the redshift we observe for light from a distant object should be related to the distance to that object. [66] [65]

- The cosmic microwave background.
  The CMB was discovered in 1965 by Arno Penzias and Robert Wilson from Bell Labs. They were working with a microwave receiver on a radio telescope, but were getting a low frequency noise from every direction they pointed the receiver. They concluded that radiation was emanating from all directions in our observable locality of the universe.[65] This was the first evidence for the CMB.

  Another interesting aspect of the CMB is a distribution of wavelengths in the centimeter and millimeter wavelengths that is characteristic of black body radiation at 2.7 K. A black body radiator is an idealized object that absorbs and emits all wavelengths of radiation, the extent of absorption and emission of a given wavelength depending on the blackbody's temperature. The Big Bang model predicts that at high temperature the universe is filled with a plasma, a blackbody radiator. This would occur as a result of an ambient temperature of about 3000K, at which hydrogen can only exist as a plasma. As the universe continued to expand the plasma began to cool, it eventually reached the temperature where electrons were able to combine with nuclei to form neutral atoms.[65] [66] Before this recombination epoch, the Universe would have been opaque due to the free electrons causing photons to scatter. However, when the free electrons were absorbed to form neutral atoms, the Universe suddenly became transparent, this is afterglow is what we observe with the cosmic microwave background.

- The relative primordial abundances of light elements (Helium 3 and 4, Deuterium, Lithium).
  To begin with, it was estimated that only a small amount of matter found in the Universe should consist of helium if stellar nuclear reactions were its only source of production, however, due to advances in spectroscopy, physicists have successfully estimated that up to 25% of the observable mass in the universe is helium.This value is too large to be explained by stellar fusion. [56] [65] The abundance of lighter nuclei such as Li is also difficult to explain by stellar nucleosynthesis; however, the Big Bang model theorizes that the very early Universe was too energetic for matter and so all matter was fully ionized and dissociated. [56]

  After a short time after Big Bang itself, the temperature of the Universe rapidly cooled from an estimated value of 10^{32} Kelvin to approximately 10^9 Kelvin. It was at this temperature, nucleosynthesis could begin. In a short time interval, protons and neutrons collided to produce elements such as deuterium, which is unable to be formed inside stellar cores because unlike helium, deuterium is a very fragile element. It gets destroyed at $10^6 K$, which is below the temperature in a stellar core, which is on the order of $10^6 - 10^8$ Kelvin. [65]

It is for these reasons that this theory is used for a framework for other predictions regarding our universe. One such prediction is that at the beginning there was once an absence of matter from the universe, only energy in the form of photons. As the universe expanded, another prediction obtained from the big bang, it cooled and hence became less

energetic and turbulent, and matter was able to form through the process: [60]

$$\gamma + \gamma \ \rightarrow p + \bar{p}. \tag{75}$$

Where γ represents the photon, p and $\bar{p}$ represents the particle and anti-particle respectively. Or in the language of Feynman diagramsSection VIII A: From looking at this interaction equal amounts of particles and anti-particle

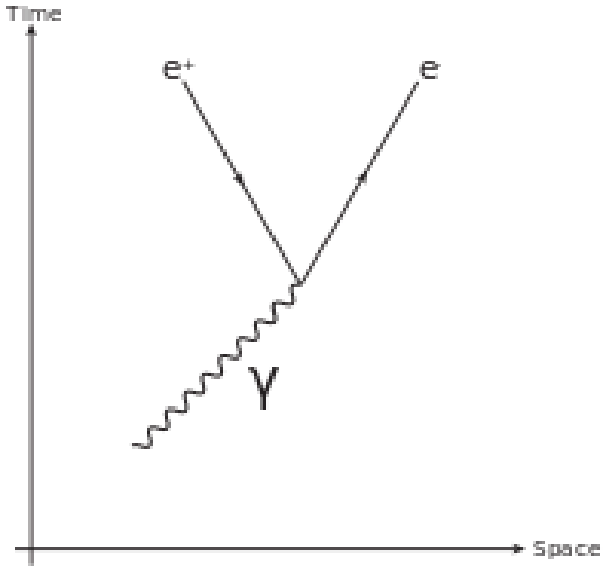

FIG. 25: Feynman diagram showing pair production from gamma ray photons

are produced and that if one were to consider these conditions alone it appears as though there should be a symmetry between matter and anti-matter. However, it is matter not anti-matter but matter that we observe out to distances of 10Mpc [56] and there exists strong evidence that this is applicable to the universe as a whole. The evidence to support this lies in the fact that there are no large localised gamma ray sources that appear to not have a source, i.e. a diffuse background. In conclusion, there exists a contradiction between the simple formulation of the big bang model and the small ratio of anti-matter to matter, currently estimated at approximately 10^{-4} [68][60]

B. Baryogenesis and Leptogenesis

The problem of the baryon asymmetry of the universe is a classic problem of particle cosmology, studies in particle physics has taught us that matter and antimatter behave essentially identically. However, cosmology teaches us that the early universe was an extremely hot, and hence energetic, environment in which one would expect equal numbers of baryons and anti baryons to be copiously produced, as described above.[68] [60] This early state of the universe stands in direct contradiction to what is observed in the universe today. Astronomical surveys and mission have shown that our universe contains no appreciable quantity of primordial antimatter. In addition, the theory of primordial nucleosynthesis allows accurate predictions of the cosmological abundances of all the light elements, while the only constraint begin that[60]:

$$2.6 \cdot 10^{-10} < \eta \equiv \frac{n_b}{n_{barb}} < 6.2 \cdot 10^{-10}, \tag{76}$$

Where:

- η is the baryon asymmetry.
- n_b/n_{barb} is the number density of baryons/anti-baryons.

- s is the entropy density.

This as been calculated from precise measurements of the relative heights of the first two microwave background acoustic peaks by the WMAP satellite [69] The baryon asymmetry can be also be expressed as:

$$0.015(0.011) < \Omega_B h^2 < 0.026(0.038), \tag{77}$$

Where:

- Ω_B is the proportional critical density in baryons.
- h h parametrizes the present value of the Hubble parameter ($h = \frac{H_0}{100(KmMpc^{-1}sec^{-1})}$)

As cosmic inflation occurred the universe cooled and hence the number of nucleons and anti-nucleons decreases[56], so long as the annihilation rate $\Gamma_{ann} \simeq n_b \langle \sigma_a v \rangle$ is larger than the expansion rate of the universe, where $\langle \sigma_a v \rangle$ is the averaged annihilation cross section. As the annihilations freeze out the anti-nucleons, being so rare, they cannot annihilate any longer. Therefore the ratios of baryons and anti-baryons becomes: [56] [69] [66]

$$\frac{n_b}{n_\gamma} \simeq \frac{n_{barb}}{n_\gamma} \simeq 10^{-18}, \tag{78}$$

which is much smaller than the required value for nucleosynthesis to occur. An initial asymmetry could thought to be imposed as an initial condition rather than an afterward mechanism, however this would violate any naturalness principle . The next section the Sakharov Criteria which must be satisfied by any particle physics theory through which a baryon asymmetry is produced[[60][68]].

C. Conditions for baryogenesis

Sakharov conditions for Baryogenesis[60], he described three processes of nature that were required for baryogenesis to occur. All of these ingredients are compatible the Standard Model. Whether or not a single mechanism can combine all of them to provide the baryon-dominated universe we see today is an open question [60].

- At least one B-number violating process.
- C and CP violation.
- Interactions outside of thermal equilibrium.

D. B-number violation

The Standard Model Lagrangian conserves B classically, but there is a global anomalies under which B- conservation could be violated. The canonical example is the sphaleron process. In electroweak gauge theory, the vacuum state is infinitely degenerate, and the different sub-states are separated by energy barriers[cite]. Through a quantum tunneling process, the system can move to a different vacuum sub-state which has nonzero baryon number.[68][60] The sphaleron process is considered to be non-perturbative, so it is not possible to draw a true Feynman diagram for illustrate the process.

It is a static solution to the electroweak field equations of the Standard Model and geometrically, a sphaleron is simply a saddle point of the electroweak potential energy[63][68]. In the standard model, processes violating baryon number convert three baryons to three anti-leptons, and related processes. This violates conservation of baryon number and lepton number, but the difference B-L is conserved. A sphaleron may convert baryons to anti-leptons and anti-baryons to leptons, and hence a quark may be converted to 2 anti-quarks and an anti-lepton, and vise versa.[60]. While it cannot be shown in the form of a Feynman diagram, due to its non-perturbative nature, Section VIII D shows an example of exchanging three leptons, one from each generation(electron, muon, tau), for nine quarks, three within each generation, and one of each color per generation. L and B are not conserved individually though the quantum number B - L is, consider the example[68]:

$$\Delta L = \Delta B = \pm 3 \tag{79}$$

$$\Delta B - \Delta L = 0 \tag{80}$$

Essentially this process generates a baryon excess out of a lepton excess. [60]

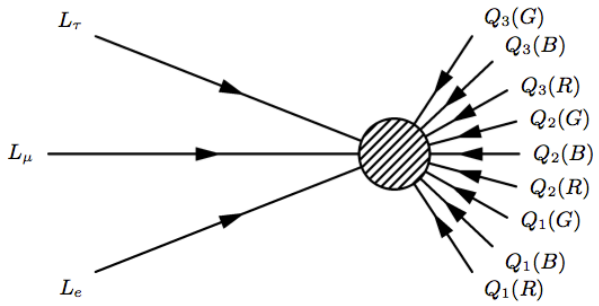

FIG. 26: The incoming quantum numbers are L = 3 and B = 0. The outgoing quantum numbers are L = 0 and B = -3.

E. Interactions outside of thermal equilibrium

Even with CP-violation working in favor of baryogenesis, there are thermodynamic considerations. The energy difference between a particle and its corresponding antiparticle is [60]:

$$\Delta E = m_{matter} + m_{matter} = 0 \tag{81}$$

At thermal equilibrium, the Boltzmann distribution dictates that there should be equal amounts of matter and antimatter. Other processes will turn any baryon asymmetry back into even numbers of baryons and anti-baryons. Thus, any baryogenesis must happen under conditions outside of thermal equilibrium.[cite] Once baryogenesis occurs, the universe returns to thermal equilibrium, this implies the conditions then must have changed such that the generated asymmetry cannot be reversed.[60] [68]

There is a natural setting for interactions outside of thermal equilibrium in the Standard Model. Consider the spontaneous electroweak symmetry breaking that happens during the electroweak phase transition which is relevant for temperatures, $T \sim 100GeV$. An analogy for this phase transition mechanic is like bubbles of steam forming inside boiling water. The inside of the bubbles, where the symmetry has broken is at thermal equilibrium with its surroundings, as are the outside of the bubbles. For the boundary this is not the case. On the inter-phase between the two phases, all interactions occur outside of the equilibrium. As the bubbles expand to cover all space and the universe cools, the results of whatever happened on the boundaries become frozen in.[60]
There are few possible mechanics to further explain this process.

1. Electroweak phase transition

his mechanism involves the three examples of the Sakharov conditions in the Standard Model above. During the electroweak phase transition, baryon-generating processes, the above mentioned sphaleron process, which took place at the inter-phase. Due to CP-violation, baryogenesis dominated over the conjugate process. After the transition ended, the temperature fell below the sphaleron mass. The baryon excess was therefore frozen in [60] Current theoretical calculations result in a much lower value of η, as shown above see Eqn.(78), than experiment. In particular, CP-violation in the quark sector may not be enough to explain the large asymmetry. It is thought that the amount of CP actually observable, and/or the branching ratio of the decay mode is not of high enough significance to explain the large asymmetry between matter and anti-matter.

2. Leptogenesis

A large lepton excess is generated through a currently unknown mechanism, and then B - L conserving processes turn this into a baryon excess directly, see Section VIII D fig.1. CP-violation in leptogenesis becomes effective CP-violation in baryogenesis. This mechanism is more attractive because CP-violation in the lepton sector is not nearly as constrained, mainly due to the fact that measuring it is much more experimentally challenging. This mechanism turns the mystery of baryogenesis into the complementary one of leptogenesis. [60]

F. C- and CP-Violations.

Baryon number alone is not sufficient to account for the matter anti-matter symmetry, if the symmetry of the universe is charge conjugation [C], then is this quantity is conserved then all B-number violation reactions: [60]

$$X \to Y + B \tag{82}$$

has the same width as the charge conjugation reaction. The quantities X and Y have a baryon number of zero, and B is a non-zero excess baryons. The conjugation reaction is as follows:

$$\Gamma(X \to Y + B) = \Gamma(\bar{X} \to \bar{Y} + \bar{B}) \tag{83}$$

Since both of the process happen as the same rate, over long time intervals the B-number is conserved. This justifies that C-Violation is a Sakharov conditions[60]
In addition to this, next consider a hypothetical process that violates B-number, $X \to q_L q_L$, which results in the creation of left-handed baryons. This then occurs at the same rate as the CP conjugate process, $X \to q_R q_R$ and hence:

$$\Gamma(X \to q_L q_L) + \Gamma(X \to q_R q_R) = \Gamma(\bar{X} \to \bar{q_L}\bar{q_L}) + \Gamma(\bar{X} \to \bar{q_R}\bar{q_R}) \tag{84}$$

In conclusion, the C-conjugate reactions have a different width, but the sum of the two will still preserve baryon number Thus, CP needs to be violated as well, so that the rate of baryogenesis exceeds that of anti-baryogenesis. With C- and CP-violation, the rate of $B - production$ can exceed that of $\bar{B} - production$.[60] [68]

IX. SEARCHING FOR EVIDENCE OF CP IN THE DIFFUSE GAMMA RAY SKY.

A. Introduction

Magnetic fields in various astrophysical settings may in fact be helical and, in the cosmological context, may provide a measure of primordial CP violation during baryogenesis.[57]
It is a safe assumption to make; that magnetic fields pervade all astronomical objects [57] [58], expanding on this; there is strong theoretical evidence, predicted by current cosmological models, to support the idea that a weak magnetic filed pervades the entire universe itself. Motivated by this idea of a pervading cosmological magnetic field with non-trivial helicity(in cosmology, a number of scenarios predict the creation of a primordial field with non-zero helicity [57]), a CP odd statistic, defined by Q, could be, theoretically evaluated be using gamma ray ray data from TeV blazars observed by Fermi satellite's instrument LAT [64].
Before an in-depth analysis can be made, foundations must first be laid by explaining certain concepts.

- Helicity.
  By definition it is the projection of a particle's spin onto the direction of its momentum as the projection of the orbital angular momentum is zero along the linear momentum. [59] Helical magnetic fields can be said to possess the property of a non-vanishing component in the direction of the current, $B(\nabla \wedge B) = 0$ and which could be being created during the electro-weak phase. [60][59]

- Blazars.
  They are what are described by the term, Active Galactic Nuclei (AGN). Which is a galaxy at a low redshift, characterised by a variable luminosity. Active galaxies, unlike our own galaxy, show an extra emission of radiation predominately in the form of massive jets. The engine powering these jets is thought to be an accreting super-massive at the galaxies centre around which gravitational energy is converted to electromagnetic radiation. [64]

The helicity of the magnetic field is related to the cosmological baryon asymmetry arising from the charge conjugation [C] and Parity [P] violation process that occurred in the young universe, which resulted processes such a mattergensis which is thought to the mechanism for the matter anti-matter asymmetry, the sign of the helicity is predicted to be left-handed i.e. the spin is opposite the linear momentum [57]. The understanding of this magnetic field would go towards defining the cosmological environment leading to an investigation to how structure would form. Results from this be be compared with observations to test the theory's effectiveness. The magnetic helicity can take on the

analogy of a screw-like distribution of magnetic field lines [59] Or in formulae form Eqn.(85), the magnetic helicity density within a large volume V, like our universe, is defined as:

$$h = \frac{1}{v}\int_V d^3x\ \vec{A}\cdot\vec{B} \tag{85}$$

Which provides a measure of the topological structure of the magnetic field.[59] Where:

- A is the electromagnetic potential of the magnetic field.
- $\vec{B} = \nabla \wedge \vec{A}$
- V is the volume element of the system.

B. Indirect and direct method's for measuring helical magnetic fields

- Indirect measurements

These involve relying on the non-helical power spectrum measurements, from this the properties of the helicitical spectrum are deduced on the bases of MHD evolution, magnetic hydromagnetic evolution.[62]
The self-similarity of the magnetic power spectrum implies that $\zeta \sim t^{1/2}$, where ζ is the magnetic field cohesion length. This then implies that H, the magnetic helicity decays as $H \sim t^{2s}$. The parameter s can be expressed as[62][61];

$$s = (\frac{\zeta_{diff}}{\zeta_H})^2. \tag{86}$$

Where:

- ζ_{diff} is the diffusion length scale.
- ζ_H is the diffusion length scale defined from the helicity power spectrum.

The actual magnetic helicity remains constant, implying that the magnetic energy decays as $Em \sim t^{-\frac{1}{2}2s}$. The parameter s is seen to be inversely proportional to the Reynold number, R_{em}, which is effectively constant throughout this regime. [62]

Another method would be to construct cross-correlations of cosmic microwave background temperature and polarisation [73]. By discussing approximations for the tensor contributions induced by helicity, their amplitude and spectral index in dependence of the power spectrum of the cosmological magnetic field. It is seen that an helical magnetic field creates a parity odd component of gravity waves inducing parity odd polarization signals. [62][59].

C. Direct Measurements

Direct measurements are the focus for this section, they can only measured by studying the propagation of polarized particles created by synchrotron radiation in the astrophysical jets of blazars. When propagating through the magnetic field the polarised particle experience the full three-dimensional effects of the magnetic field. It is due to the polarised nature of the synchrotron that leaves it sensitive to magnetic helicity. [57] [64]. In such situations, the velocity of electrons in the jets is known and this additional information is crucial to the determination of helicity. In other situations, it is much harder to find the helicity. For example, Faraday rotation only provides an estimate of the line of sight component of the magnetic field. Even by observing the Faraday rotation from different sources, the information is insufficient to estimate the helicity. An estimate of the helicity necessarily requires sensitivity to all components of the magnetic field, i.e. the three-dimensional effects felt. [70]
Obtaining information about the magnetic field from the gamma rays is not a straight forward process, firstly TeV gamma rays are produced blazars. The TeV photon from the blazar jets then interacts with the background radiation of the blazar, creating an electron-positron pair. This electron-positron pair then propagates in the cosmic magnetic field until it up-scatters, by inverse-Compton scattering, the cosmic microwave background photons to produce GeV photons and these photons carry the information about the helicity of the intervening magnetic field [64] A key note to regard is that while the microwave background is most widely known of the cosmic backgrounds because the radiation intensity peaks at these wavelengths, this does not mean backgrounds of other wavelengths do not exist. This observed diffuse gamma ray background is theorised to hold information about the cosmological helical magnetic field and CP violation in the early universe. [65] An odd parity statistic, Q, can be calculated from the diffuse gamma ray background as this background is sensitive to the helicity of an intervening magnetic field. The odd parity statistic could be evaluated from the Large Area Telescope (LAT) which is on board the Fermi satellite.[57]

D. Fermi LAT's method of gamma ray detection

The Large Area Telescope (LAT), the primary instrument on the Fermi Gamma-ray Space Telescope mission, it is an imaging, wide field-of-view, high-energy gamma ray telescope, covering the energy range from below 20 MeV to more than 300 GeV [71] The Large Area Telescope is a pair-conversion telescope, this process forms the basis for the underlying measurement principle by providing a unique signature for gamma rays, which distinguishes them from charged cosmic rays whose flux is as much as 10^5 times larger, and allowing a determination of the incident photon directions via the reconstruction of the trajectories of the resulting $e+e-$ pairs. Incident radiation first passes through an anti-coincidence shield, which is sensitive to charged particles, then through thin layers of high-Z material, were Z is the neutron number, called conversion foils. Photon conversions are facilitated in the field of a heavy nucleus. After a conversion, the trajectories of the resulting electron and positron are measured by particle tracking detectors, and their energies are then measured by a calorimeter.[72] [71]

It consists of a precision tracker and calorimeter, each consisting of a 4 x 4 array of 16 modules, a segmented anti-coincidence detector that covers the tracker array, and a programmable trigger and data acquisition system. Each tracker module has a vertical stack of 18 (x, y) tracking planes, including two layers $(xandy)$ of single-sided silicon strip detectors and high-Z converter material (tungsten) per tray. Every calorimeter module has 96 CsI(Tl) crystals, cesium iodide crystals. These crystals arranged in an eight-layer hodoscopic configuration with a total depth of 8.6 radiation lengths, giving both longitudinal and transverse information about the energy deposition pattern.[cite] The on-board calorimeter can measure the three-dimensional profiles of showers due to the hodoscopic configuration.[72]

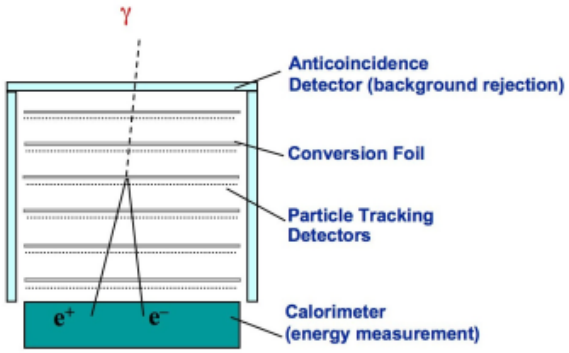

FIG. 27: Cross-section of LAT

E. Gamma ray spirals in a helical magnetic field

Assume a position located within the particle jet opening angle of a blazar but are off-axis. A photon of energy $E1 \sim 1TeV$ from the blazar propagates a distance, $D_{E1} \sim 100Mpc$ and then scatters with an extragalactic background light photon to produce an electron-positron pair [cite 1,14]. As the electron positron trajectories are bent due to the Lorentz force by a magnetic field, the GeV photon cascade carries information about the structure of the cosmological magnetic field and, after a typical distance of about 30 kpc, up-scatters, via inverse Compton scattering, a cosmic microwave background photon, that arrives to an observer at the vectorial position denoted by ϑ_1, which lies on the observer plane. At the same time another photon, with energy E_2, arrives at a second vectorial position, ϑ_2 in the same plane. [57] [59] The ϑ term can be expressed as:

$$\vartheta \equiv \frac{\delta x_i - \delta x_f}{D_e} \tag{87}$$

Where:

- δx_f is $\delta x(t) att = t_f$, final time, i.e. when the particle up-scatters, $\delta x(t)$ is the position deviations induced by the magnetic field [59]
- D_e is the distance traveled.

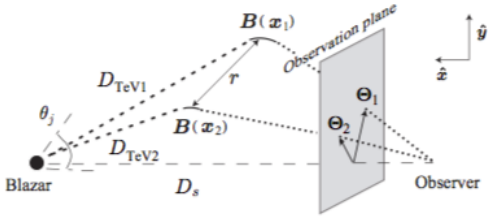

FIG. 28: Events at two different energies sample the magnetic field in regions of a certain size, D_e [59]

This can be shown in Section IX E. Working through the mathematics, which is done out fully in [59], an approximation of the position of the blazar using the position of the highest energy photon and relevant correlator. The correlator in this case is is the helical correlator, $G(E_1, E_2)$, as this is a measure of CP violation[73]:

$$G(E_1, E_2) = \langle \vartheta(E_1) \wedge \vartheta(E_2) \cdot \hat{x} \rangle \tag{88}$$

Where:

- $\hat{x}$ is perpendicular to the plane of observation and points in the direction of te source.
- The correlator is defined only if the blazar is visible, detectable, as the vectors ϑ_1, ϑ_2 originate at the line of sight intersects the observational plane. [59]

However, diffuse gamma rays are observed on a sphere, i.e. the sky, and not on a plane and so the statistic $G(E1, E2; E3)$ needs to be modified in accordance to this, so the statistic becomes:

$$Q'(E_1, E_2, E_3) = \langle (n(E_1)) - n(E_3) \wedge (n(E_2 - n(E_3) \cdot E_3) \rangle = \langle n(E_1) \wedge n(E_2) \cdot n(E_3) \rangle \tag{89}$$

Where, $n(E)$ denotes the unit vector to the location of the photon with energy, E, on the sky. the highest energy E3 photons approximately represent the source directions. Lower energy (E1 and E2) photons in patches of some radius R around the position of the E3 photon are more likely to be from the same source [57]. See Section IX E for illustration, showing that gamma rays distributed on the sky. This figure demonstrates whether the directed curves from E3 to E2 to E1 are bent to the left or to the right, i.e. are the photons of decreasing energy in patterns of left-handed or right-handed spirals? A positive value of the statistic Q implies that there is an excess of right-handed spirals in the gamma ray sky and a negative value implies a left-handed excess.[57] The final expression, which can

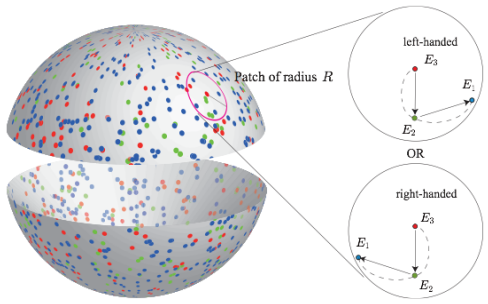

FIG. 29: Events at two different energies sample the magnetic field in regions of a certain size, D_e[57]

be see [57][59], becomes:

$$Q(E_1, E_2, E_3, R) = \frac{1}{N_1 N_2 N_3} \sum_{i=1}^{N-1} \sum_{j=1}^{N-2} \sum_{k=1}^{N-3} W_R(n_i(E_1) \cdot n_k(E_3)) W_R(n_j(E_2) \cdot n_k(E_3)) n_i(E_1) \wedge n_j(E_2) \cdot n_k(E_3) \tag{90}$$

Where the indices refer to the different photons and W_R is a top hat window function.

$$W_R(cos\alpha) = \begin{cases} 1 & for \;\; \alpha \leq \;\; R \\ 0, & otherwise \end{cases} \tag{91}$$

F. Evaluation of the theory

The above processes, though theoretically sound, possess certain difficulties in proving experimentally. The mathematics assume, for it to work, that the electron-position pair interact with the cosmological magnetic field, which is helical in nature.[61] [58] However, it would not be until the strength of the field was determined, it would not be known if the bending of the particle's trajectory is due to the magnetic field induced by the TeV blazar; who's magnetic field also exhibits a corkscrew field line pattern, due to its rotation. Recent gamma ray observations suggest the existence of cosmological magnetic fields of approximately 10^{-16} Gauss. [61] So in conclusion, again considering the below equation [59]:

$$h = \frac{1}{v}\int_V d^3x\ \vec{A}\cdot\vec{B}. \tag{92}$$

Magnetic helicity is odd under CP transformations as A and B are odd under C-symmetry , while A is even but B is odd under P, parity [73]. Non-zero magnetic helicity is predicted in scenarios in which cosmic baryogenesis and magnetogenesis occur concurrently during a cosmological phase transition, the electro-weak. Then the magnetic helicity density is related to the cosmic baryon number density and the CP violation responsible for the excess of matter over antimatter also provides helicity to the magnetic field. [73][57] [59]

X. ACKNOWLEDGEMENTS

We would like to thank Professors John Quinn, Peter Duffy and Sheila McBreen for their guidance and explanations of many aspects of this review including understanding of difficult astrophysical concepts which were previously unknown to us.

---

[1] Hilary Greaves and Terugi Thomas - "The CPT Theorem" - April 2012, http://arxiv.org/abs/1204.4674
[2] Frank Close, "The new cosmic onion," London: Taylor & Francis, 2006, pages 149 - 161
[3] David Griffiths, "Introduction to Elementary Particles" Wiley-VCH, 2004, pages 301 - 330
[4] Kobayashi and Maskawa, "CP-Violation in the Renormalizable Theory of Weak Interactions," Progress of Theoretical Physics, Vol. 49, No. 2, February 1973
[5] C. Jarlskog, "Commutator of the quark mass matrices in the standard electroweak model and a measure of maximal CP nonconservation," Phys. Rev. Lett. 55, 1039-1042 (1985)
[6] J. Buras and R. Fleischer,"Quark Mixing, CP Violation and Rare Decays After the Top Quark Discovery" High Energy Phys. 15:65-238, 1998
[7] M. Baak - "Measurement of the CKM angle γ with charmed B^0 decays," - SLAC-R-858, THESIS-BAAK, 2007
[8] http://pi.physik.uni-bonn.de/~brock/teaching/vtp$_$ss03/chapter4$_$html/node2.html
[9] N. Cabibbo - "Unitary Symmetry and Leptonic Decays" - Phys. Rev. Lett. 10, 531-533, 1963
[10] Glashow, Iliopoulos and Maiani - "Weak Interactions with Lepton-Hadron Symmetry," - Physical Review D, vol. 2, Issue 7, pp. 1285-1292, 1970
[11] Wolfenstein - "Parametrization of the Kobayashi-Maskawa Matrix" Phys. Rev. Lett. 51, 19451947, 1983
[12] Robert Mann - "An introduction to particle physics and the standard model" - CRC Press, 2010, page 413-416
[13] J. H. Christenson, J. W. Cronin, V. L. Fitch, and R. Turlay - "Evidence for the 2π Decay of the K_2^0 Meson" - (1964) Phys. Review letters, vol. 13, issue 4
[14] J. Beringer et al. (Particle Data Group) - "2013 Review of Particle Physics" - Phys. Rev. D86, 010001 (2012) and 2013 partial update for the 2014 edition
[15] B.R Martin, G. Shaw - "Particle Physics, Third Edition" - Wiley(2008)
[16] Tatsuya Nakada - "Review on CP Violation" - arXiv:hep-ph/9312290v1 15 Dec 1993
[17] http://large.stanford.edu/courses/2008/ph204/coleman1/
[18] KTeV Collaboration - "Measurements of Direct CP Violation, CPT Symmetry, and Other Parameters in the Neutral Kaon System" - arXiv:hep-ex/0208007v1 6 Aug 2002
[19] Donald H. Perkins - "Introduction to High Energy Physics" - Cambridge University Press, 4th edition
[20] Giancarlo DAmbrosio and Gino Isidori - "CP violation in Kaon Decays" - arXiv:hep-ph/9611284v1 8 Nov 1996
[21] Gjesdal, S. et al. - "A Measurement of the K(L)-K(s) Mass Difference from the Charge Asymmetry in Semileptonic Kaon Decays" - Phys.Lett. B52 (1974) 113 Print-74-1358 (CERN)
[22] http://www.hep.phy.cam.ac.uk/thomson/partIIIparticles/handouts/Handout_12_2011.pdf
[23] B. Aubert - "Measurement of the $B^0 - \bar{B}^0$ Oscillation Frequency with Inclusive Dilepton Events" - Phys. Rev. Lett. Volume 88, Number 22, 3 June 2002

[24] Sciolla - "Recent measurements of $\sin 2\beta$ at BaBar Nuclear Physics B - Proceedings Supplements" - Volume 156, Issue 1 June 2006

[25] Boos - "The Gold-plated mode revisited:sin(2β) and $B^0 \to J/\Upsilon K_S$ in the Standard Model" - Phys. Rev. D70 (2004) 036006

[26] The BABAR Collaboration - "Technical Design Report" - SLAC-R-0457, 1995

[27] The BABAR Collaboration -"The BABAR Detector" - Nucl. Instrum. Meth. A 479:1-116, 2002

[28] Long - "Impact of tag-side interference on time-dependent CP asymmetry measurements using coherent $B^0\bar{B}^0$ pairs" - Phys. Rev. D 68, 034010 2003

[29] D. Perepelitsa - "Measuring the CKM angle γ at the B factories" - Columbia University, `http://phys.columbia.edu/~dvp/dvp-gamma.pdf`, 2010

[30] H. LI - "Penguin pollution in the $B^0 \to J/\psi K_S$ decay" - JHEP 0703:009, 2007

[31] B. Aubert - "Improved Measurement of CP Asymmetries in $B^0 \to (c\bar{c})K^{0*}$ Decays" - Phys. Rev. Lett. 94:161803, 2005

[32] E. Baeberio - "Averages of $b-$hadron properties at the end of 2005" - FERMILAB-FN-0814-E, hep-ex/0603003, 2006

[33] `http://pdg.lbl.gov/2011/reviews/rpp2011-rev-cp-violation.pdf`

[34] AJ. Buras - "Weak Hamiltonian, CP Violation and Rare Decays" - TUM-HEP-316, 1998

[35] `http://www.phys.hawaii.edu/superb04/talks/Kelsey.pdf`

[36] `http://hep.ucsb.edu/people/claudio/Vancouver.pdf`

[37] A. Ruland - "Performance and Operation of the BABAR Calorimeter" - Journal of Physics: Conference Series 160 (2009) 012004

[38] B. Aubert - "Time-integrated and time-dependent angular analyses of $B \to J/\psi K\pi$: A measurement of $\cos 2\beta$ with no sign ambiguity from strong phases" - Phys. Rev. D 71. 3. 032005 2005 February

[39] `http://cds.cern.ch/record/1106345/files/CERN-THESIS-2008-044.pdf`

[40] `http://pprc.qmul.ac.uk/~bona/ulpg/cpv/lecture3.pdf`

[41] E. Galvez - "Interference with correlated photons" - American Journal of Physics, Volume 73, Issue 2, 2004

[42] The BaBar Collaboration - "Evidence for $D^0\bar{D}^0$ Mixing" - `http://arxiv.org/abs/hep-ex/0703020v1` 1 Apr 2007

[43] The Belle Collaboration - "Evidence for $D^0\bar{D}^0$ Mixing" - arXiv:hep-ex/0703036v2 1 Apr 2007

[44] `http://inspirehep.net/record/1209003/files/mix-rick.png`

[45] Giulia Casarosa for the BABAR Collaboration - "Studies of CP Violation and Mixing in the D Mesons decays from BABAR" - Journal of Physics: Conference Series 335 (2011) 012043 doi:10.1088/1742-6596/335/1/012043

[46] Kevin Maguire, C. Parkes, M. Vesterinen - "New tagged $D^0 \to hh\pi^0$ stripping lines" - LHCb-INT-2013-049 October 1, 2013

[47] The BaBar Collaboration - "Improved measurement of the CKM angle γ in $B^\pm \to D^{(*)}K^{(*)\mp}$ decays with a Dalitz plot analysis of D decays to $K^0_S\pi^+\pi^-$ and $K^0_SK^+K^-$" - arXiv:0804.2089v2 [hep-ex] 7 Aug 2008

[48] The LHCb Collaboration - "Measurements of indirect CP asymmetries in $D^0 \to K^+K^-$ and $D^0 \to \pi^+\pi^-$"- arXiv:1310.7201v1 [hep-ex] 27 Oct 2013

[49] François Goffinet, CP3 Seminar, Unitè de Physique Thèorique et Mathèmatique, U.C.L., December 2003

[50] Yoav Achiman - "Spontaneous CP Violation in SUSY" - Physics Letters B, March 2007

[51] Peter Szekeres - "A Course in Modern Mathematical Physics" - Cambridge University Press, 2004

[52] John Baez and John Huerta - "The Algebra of Grand Unified Theories" - Bulletin of the American Mathematical Society, vol 47, May 4 2010

[53] Howard E. Haber and Ze'ev Surujon - "Group-theoretic Condition for Spontaneous CP Violation" - Physical Review D, Volume 86, Issue 7, October 2012

[54] Bernard de Wit and Eric Laenen - "Field Theory in Particle Physics" - Lecture Notes, Universiteit Utrecht, 2009 `http://www.staff.science.uu.nl/~wit00103/ftip/Ch11.pdf`

[55] Paul H. Frampton and Masayasu Harada - "Kaon Spontaneous CP Violation Reevaluated" - Physical Review D, Volume 59, Issue 1, March 1998

[56] *Subir Sarkar*- Big Bang nucleosynthesis and physics beyond the Standard Model.

[57] *Hiroyuki Tashiro, Wenlei Chen, Francesc Ferrer, and Tanmay Vachaspati*- Search for CP Violation in the Gamma Ray Sky

[58] *R. Durrer and A. Neronov*- Cosmological magnetic fields: Their generation, evolution and observation- arXiv:1303.7121.

[59] *T. Kahniashvili and T. Vachaspati*- On the detection of magnetic Helicity-astro-ph/0511373-(2006)

[60] *D*ennis V. Perepelitsa. http://phys.columbia.edu/ dvp/dvp-sakharov.pdf

[61] *H. Tashiro and T. Vachaspati,* Estimate of the primordial magnetic field helicity-Phys. Rev. D 87, 123527 (2013).

[62] *L. Campanelli,* Scaling Laws in Magnetohydrodynamic Turbulence -astro-ph/040705- (2004).

[63] *Andrew J. Long, Eray Sabancilar, and Tanmay Vachaspati*- Leptogenesis and primordial magnetical fields-(2013).

[64] *Andrii Neronov and Ievgen Vovk*- Evidence for strong extragalactic magnetic fields from Fermi observations of TeV blazars - Data Centre for Astrophysics (ISDC), Geneva Observatory Ch. d'Ecogia 16.

[65] *Cambrige cosmology*- http://www.damtp.cam.ac.uk/research/gr/public/bb_pillars.html

[66] *h*ttp://burro.astr.cwru.edu/stu/advanced/cosmos_bigbang.html

[67] *Kishore Padmaraju*- Faraday Rotation- Department of Physics and Astronomy, University of Rochester,

[68] *Mark Trodden*- Baryogenesis and Leptogenesis- SLAC Summer Institute, 2004.

[69] *Wayne Hu and Martin White* The cosmic symphony- Scientific america.

[70] *Kishore Padmaraju*- Faraday Rotation- Department of Physics and Astronomy, University of Rochester.

[71] *http://fermi.gsfc.nasa.gov/ssc/*

[72] *M. Ackermann, M. Ajello, A. Allafort et al.* The First Fermi-LAT Catalog of Sources Above 10 GeV.
[73] *Hiroyuki Tashiro and Tanmay Vachaspati-* Cosmology magnetic field correlators from blazar induced cascades.